Generation and Characterization of Structured Partially Coherent Light

Paulo Henrique Souto Ribeiro
GIQSUL – Department of Physics
Federal University of Santa Catarina
Florianópolis

February, 2025


WORLD MAP
ARCTIC OCEAN
Green Land (Denmark)
Baffin Bay
Beaufort Sea
Bering Sea
Alaska (U S A)
Canada
Hudson Bay
Labrador Sea
Gulf of Alaska
NORTH PACIFIC OCEAN
NORTH ATLANTIC OCEAN
N
United States of America
Bermuda (UK)
Tropic of Cancer
Hawaii Island (USA)
Mexico
Gulf of Mexico
Cuba
Haiti
Dominican Rep.
Puerto Ruca (US)
St.Kitts & Nevis
Antigua & Barbuda
Domanica
St.Lucia
Barbados
Trinidad & Tobago
Grenada
Jamaica
Caribbean Sea
Belize
Guatemala
Honduras
El Salvador
Nicaragua
Costa Rica
Panama
Venezuela
Guyana
Suriname
French Guiana
Colombia
Ecuador
Galapagos (Ecuador)
Equator
Kiribati
Tuvalu
Samoa
French Polynesia
Tonga
Tropic of Capricon
Peru
Brazil
Bolivia
Paraguay
Uruguay
Chile
Argentina
Easter (Chile)
Trindade (Bra.)
SOUTH PACIFIC OCEAN
SOUTH ATLANTIC OCEAN
Falkland Islands (U.K.)
South Georgia (U.K.)
South Sandwich (U.K.)
Weddell Sea
Antarctica
Map is not to Scale
infoandopinion.com
Prime Meridian
0°
W
E
Jan Mayen (Norway)
Svalbard (Norway)
Norwegian Sea
Iceland
Faroe islands (Denmark)
United Kingdom
Ireland
Denmark
Norway
Sweden
Finland
Estonia
Latvia
Lithuania
Belarus
Poland
Germany
Ukraine
France
Liechtenstein
San marino
Monaco
Andora
Spain
Portugal
Vatican City
Morocco
Romania
Bulgaria
Turkey
Mediterranean Sea
Malta
Tunisia
Canary Island (Spain)
Western Sahara
Algeria
Libya
Egypt
Mauritania
Mali
Niger
Chad
Sudan
Senegal
The Gambia
Guinea-Bissau
Guinea
Sierra Leone
Liberia
Côte d'Ivoire
Togo
Nigeria
Central African Rep.
Cameroon
Gabon
Congo
Demo.Rep. of the Congo
Ascension (U.K.)
Sao Tome & Principe
Angola
Zambia
Namibia
Botswana
Zimbabwe
Mozambique
eSwatini
Lesotho
South Africa
St. Helena (U.K.)
Eritrea
Ethiopia
South Sudan
Somalia
Uganda
Kenya
Rwanda
Burundi
Tanzania
Malawi
Comoros
Madagacar
Mauritius
Reunion(Fr.)
Sychelles
Djibouti
Yemen
Oman
Saudi Arabia
U.A.E
Bahrain
Qatar
Kuwait
Iraq
Iran
Syria
Jordan
Israel
Georgia
Armenia
Azerbaijan
Black Sea
Caspian Sea
Red Sea
Arabian Sea
Barents Sea
Kara Sea
Novaya Zemlya
Franz Josef Land
October revolution
Laptev Sea
Kotelny
East Siberian Sea
Russia
Kazakhistan
Aral Sea
Uzbekistan
Turkmenistan
Kyrgyzstan
Tajikistan
Afganistan
Pakistan
India
Nepal
Bhutan
Bangladesh
Bay of Bangal
lakshadweep (In.)
Maldives
Sri Lanka
Andaman&Nicobar Islands(In.)
Mongolia
China
North Korea
South Korea
Sea of Japan
Japan
Sea of Okhotsk
East China Sea
Taiwan
Myanmar
Thailand
Laos
Vietnam
Campodia
Philippine Sea
Philippines
Brunei
Malaysia
Singapore
Sumatra
Java
Indonesia
Timoe-Leste
Papua New Guinea
Cocos Island(Aus.)
Christmus Island(Aus.)
INDIAN OCEAN
PACIFIC OCEAN
Northern Mariana Islands (U.S.)
Guam(U.S.)
Palau
Marshall Islands
Federated states of Micronesia
Nauru
Soloman Islands
Wallis& Futuna(Fr.)
Coral Sea
Vanuatu
Fiji
New Cledonia (Fr.)
Australia
Great Australian Bight
Tasmania
Tasman Sea
New Zealand
SOUTHERN OCEAN
1.Netherlands
2.Belgium
3.Luxembourg
4.Switzerland
5.Slovenia
6.Croatia
7.Bosnia and Herzegovina
8.Czechia
9.Slovakia
10.Austria
11.Hungary
12.Serbia
13.Moldova
14.North Macedonia
15.Albania
16.cyprus
17.Lebanon
18.Palastinian Territories
19.Burkina Faso
20.Ghana
21.Benin
22.Equatorial Guinea


Santa Catarina
AMAZONAS
PARÁ
MARANHÃO
CEARÁ
RIO GRANDE DO NORTE
PARAÍBA
PERNAMBUCO
ALAGOAS
SERGIPE
PIAUÍ
BAHIA
TOCANTINS
ACRE
RONDÔNIA
MATO GROSSO
BRASIL
GOIÁS
BRASÍLIA
MINAS GERAIS
ESPÍRITO SANTO
RIO DE JANEIRO
SÃO PAULO
MATO GROSSO DO SUL
PARANÁ
SANTA CATARINA
RIO GRANDE DO SUL
PERU
BOLÍVIA
LA PAZ
CHILE
PARAGUAI
ARGENTINA
URUGUAI
BUENOS AIRES
OCEANO PACÍFICO
OCEANO ATLÂNTICO
Trópico de Capricórnio
Manaus
Belém
São Luís
Fortaleza
Natal
João Pessoa
Recife
Maceió
Aracaju
Salvador
Teresina
Palmas
Porto Velho
Rio Branco
Cuiabá
Campo Grande
Goiânia
Belo Horizonte
Vitória
Rio de Janeiro
São Paulo
Curitiba
Florianópolis
Porto Alegre
Núcleos Urbanos
CAPITAL DE PAÍS
Capital de Estado
Sedes Municipais
Vias de Acesso
rodovias pavimentadas
terra
ferrovias
Limites
estadual
internacional
120 0 240 km
Projeção Policônica
Meridiano de Referência: -54° W. Gr
Paralelo de Referência: 0°
N

Florianópolis, SC

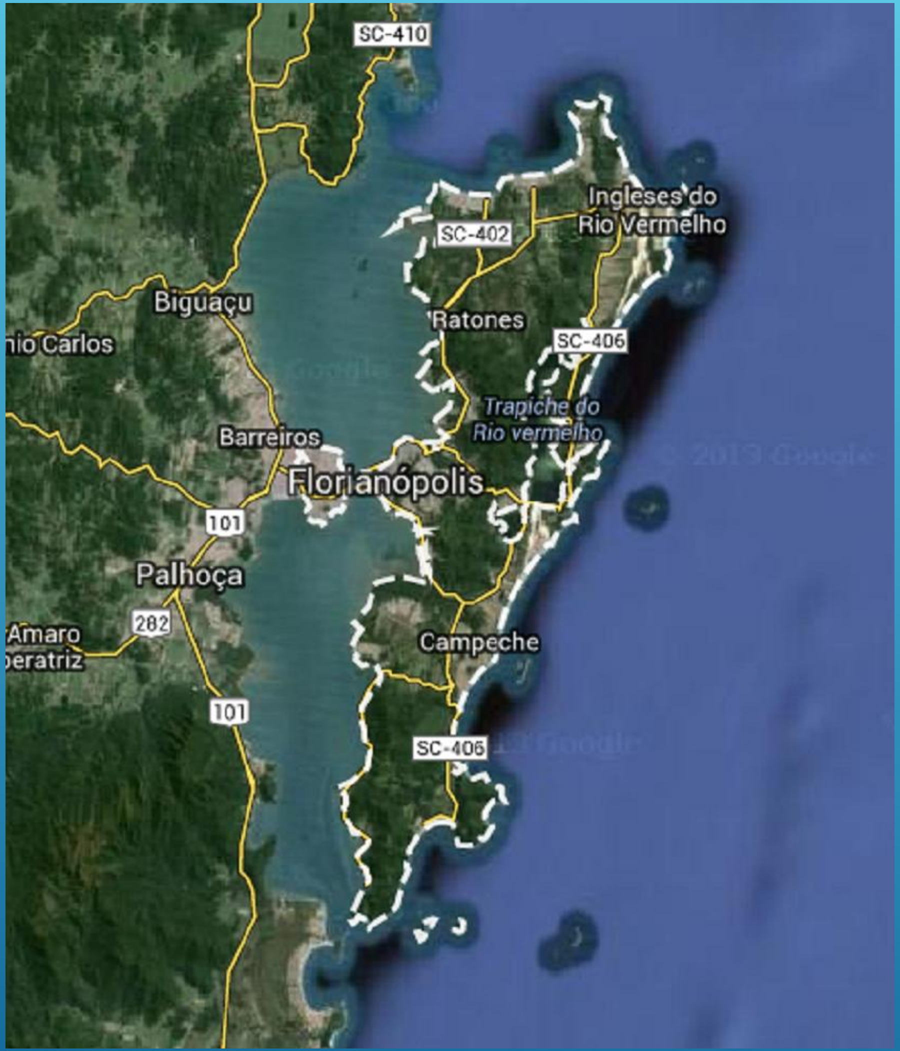

Federal University of Santa Catarina
UFSC

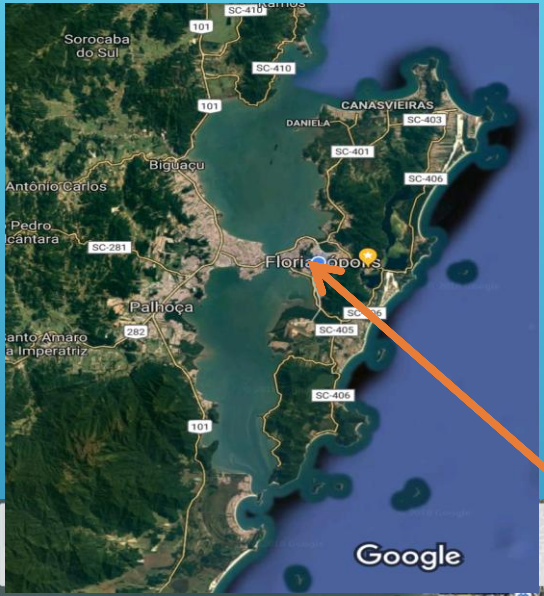

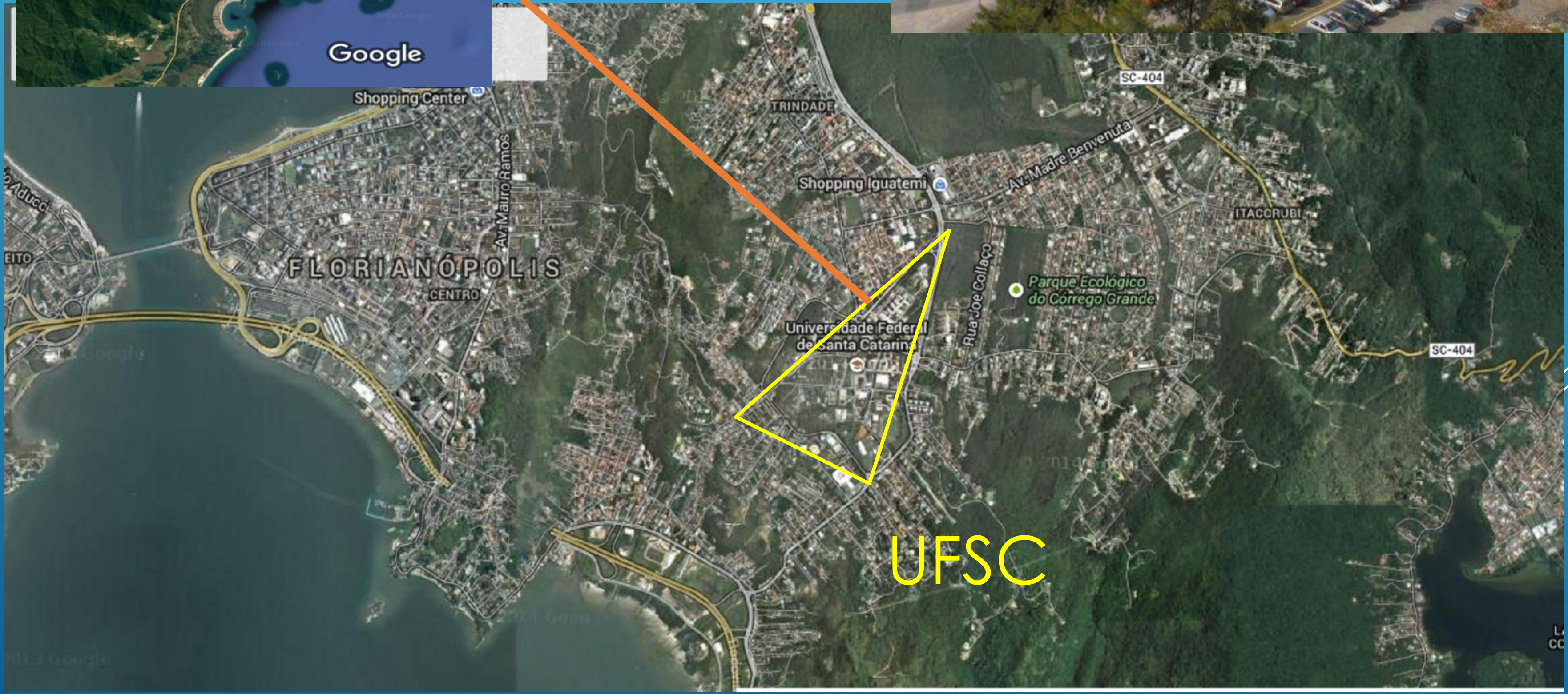

GIQSUL at UFSC
Group of Quantum Information

Quantum Optics Laboratory

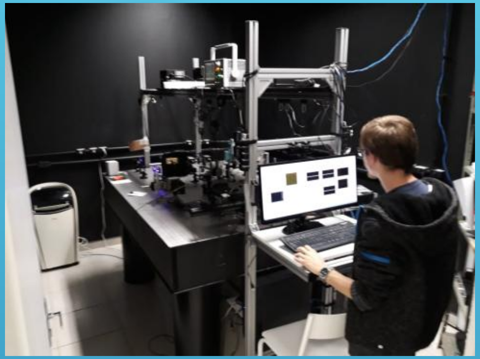

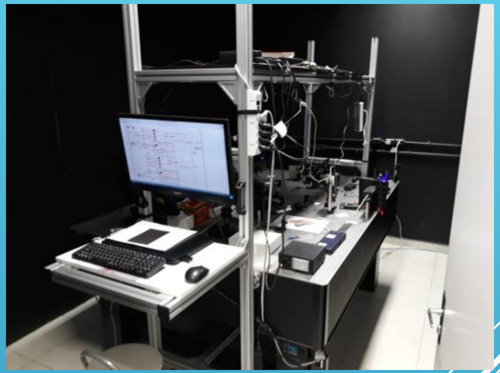

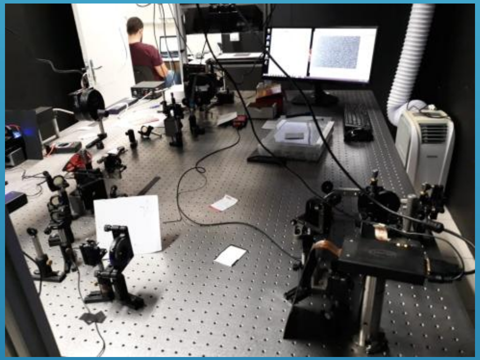

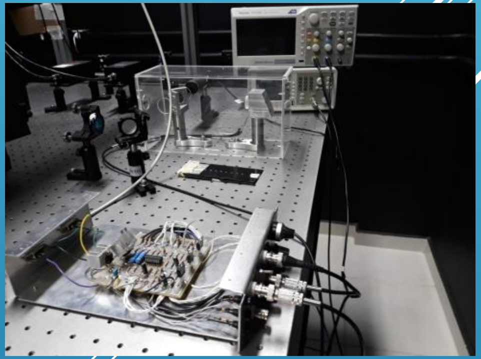

Optical Processing Laboratory

GIQSUL Research

- Transverse Spatial Entanglement with Parametric Downconversion
  Spatial correlations in parametric down-conversion, Walborn et al., Physics Reports 495, 87-139 (2010)

- Quantum Computing Theory (Duzzioni team)
  Quantum computation in continuous time using dynamic invariants, Sarandi et al., Physics Letters A, 375, 3343-3347 (2011)

- Nonlinear Optics
  Conservation of orbital angular momentum in stimulated downconversion, Caetano et al. Phys. Rev. A 66, 041801(R) (2002)

- Optical Processing
  An optical processor for matrix-by-vector multiplication: an application to the distance geometry problem in 1D, Hengeveld et al. Journal of Optics 24, 015701 (2021)

Outline

- Introduction to optical coherence
- The Gaussian Schell Model Beam (GSM)
- The Twisted Gaussian Schell Model Beam (TGSM)
- Motivation for TGSM beams
- Generation of TGSM beams
- Quantum effects with TGSM beams
- StimPDC with TGSM beams
- Conclusions and perspectives

Temporal and transverse spatial coherence

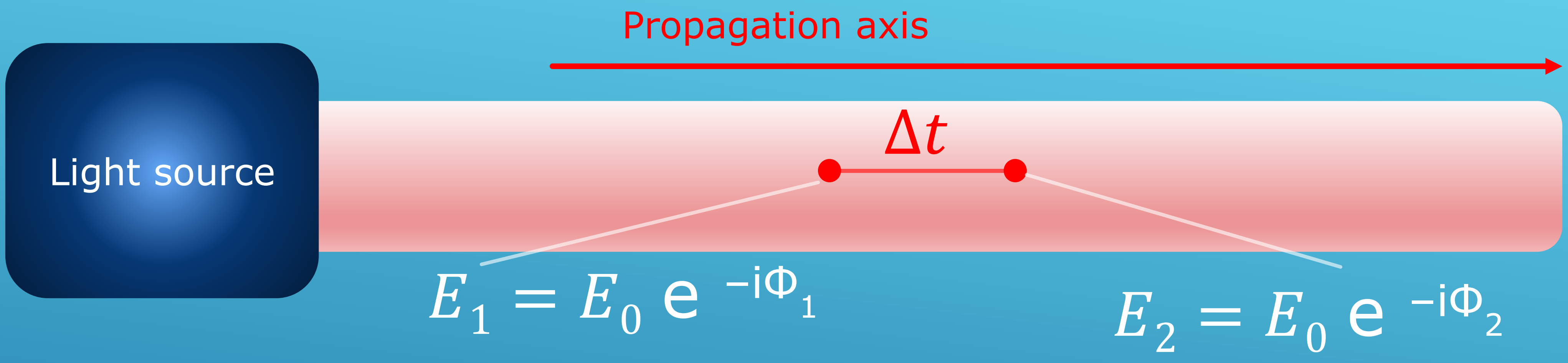

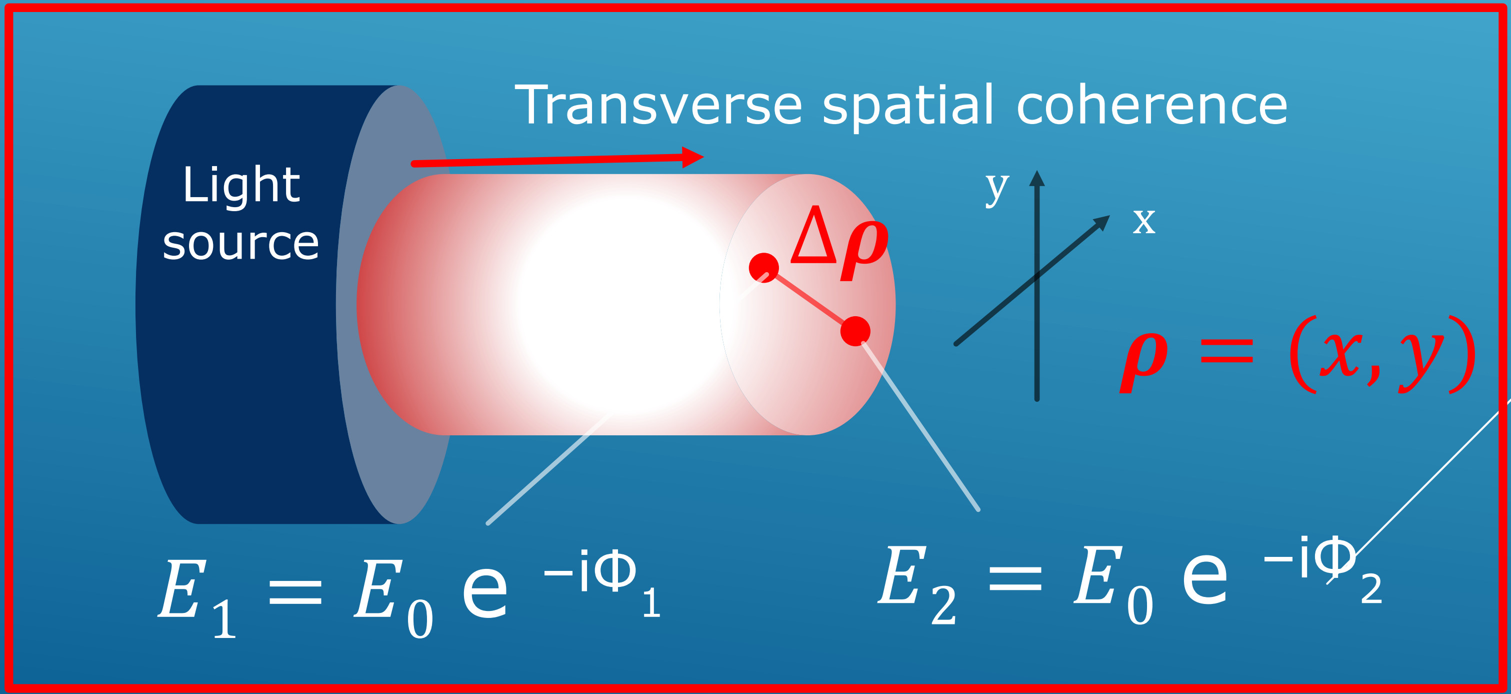

Measuring transverse spatial coherence with double-slit interference

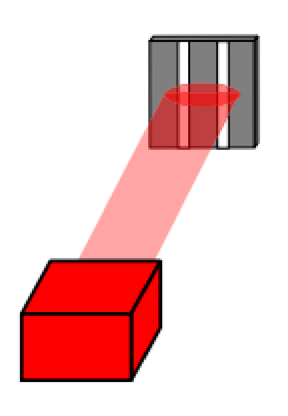

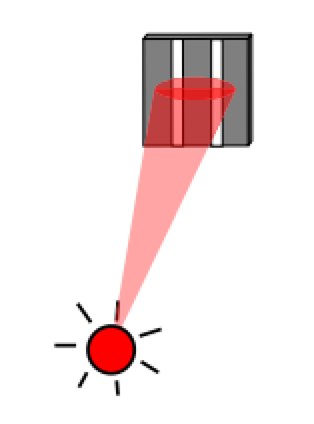

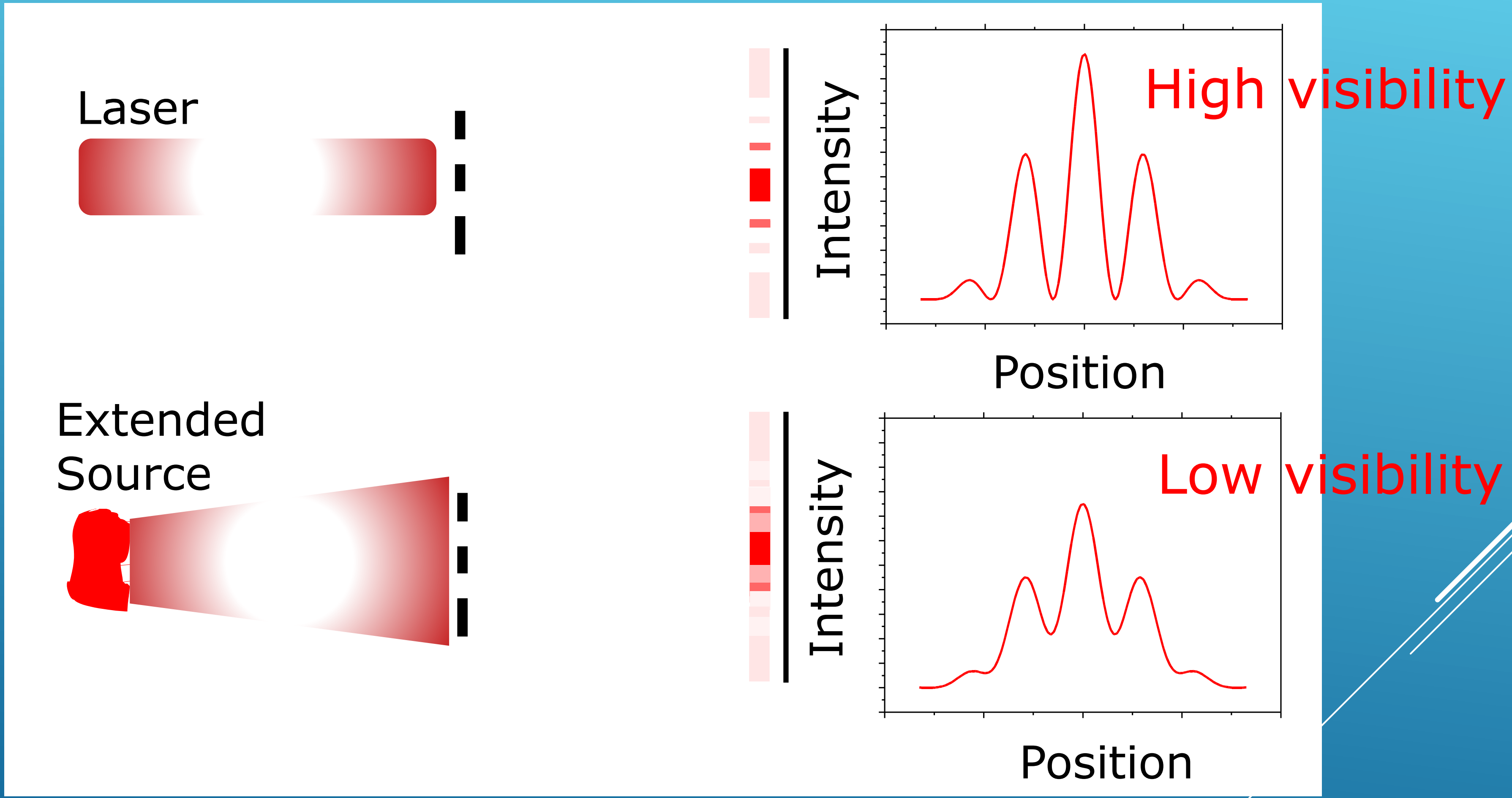

Constrast or visibility => $|\mu_{12}| = (I_{max} - I_{min})/(I_{max} + I_{min})$

Coherence and Double-slit interference

Almost monochromatic light ~ single frequency

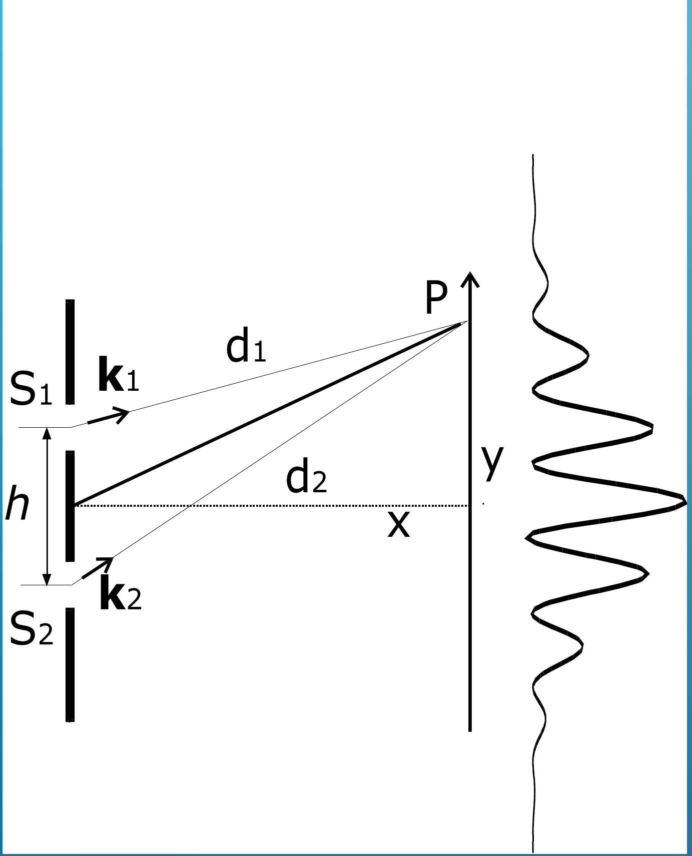

Intensity distribution

$$I(p) = I_0(y)(1 + |\mu_{12}| \cos[k(d_2 - d_1) + \varphi])$$

$$k = 2\pi/\lambda$$

$$d_1 = \sqrt{x^2 + \left(y - \frac{h}{2}\right)^2} \; ; d_2 = \sqrt{x^2 + \left(y + \frac{h}{2}\right)^2}$$

μ_{12} Normalized degree of mutual coherence

Van Cittert-Zernike theorem

Cross spectral density

$$\mu_{12} = \frac{\overbrace{\langle E_1(x_1, y_1) E_2{}^*(x_2, y_2)\rangle}}{\int_\sigma dx_0 dy_0 I(x_0, y_0)}$$

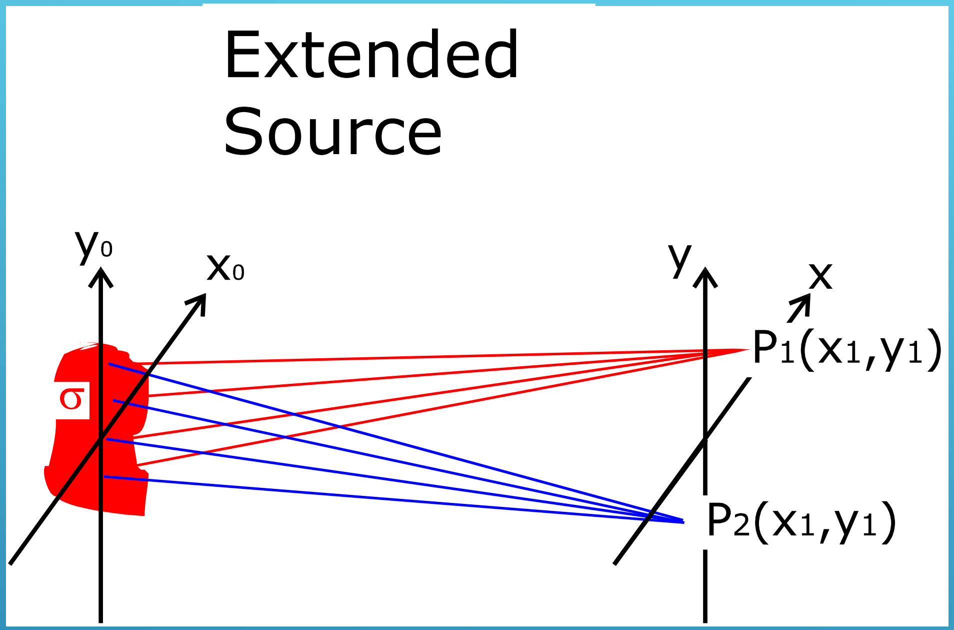

$$\mu_{12}[(x_2 - x_1), (y_2 - y_1)] = \frac{e^{i\alpha_{12}} \int_\sigma dx_0 dy_0 I(x_0, y_0) e^{i\frac{k}{R}[x_0(x_2 - x_1) + y_0(y_2 - y_1)]}}{\int_\sigma dx_0 dy_0 I(x_0, y_0)}$$

Van Cittert-Zernike theorem

$$\mu_{12}[(x_2 - x_1),(y_2 - y_1)] = \frac{e^{i\alpha_{12}} \int_\sigma dx_0 dy_0 I(x_0, y_0) e^{i\frac{k}{R}[x_0(x_2-x_1)+y_0(y_2-y_1)]}}{\int_\sigma dx_0 dy_0 I(x_0, y_0)}$$

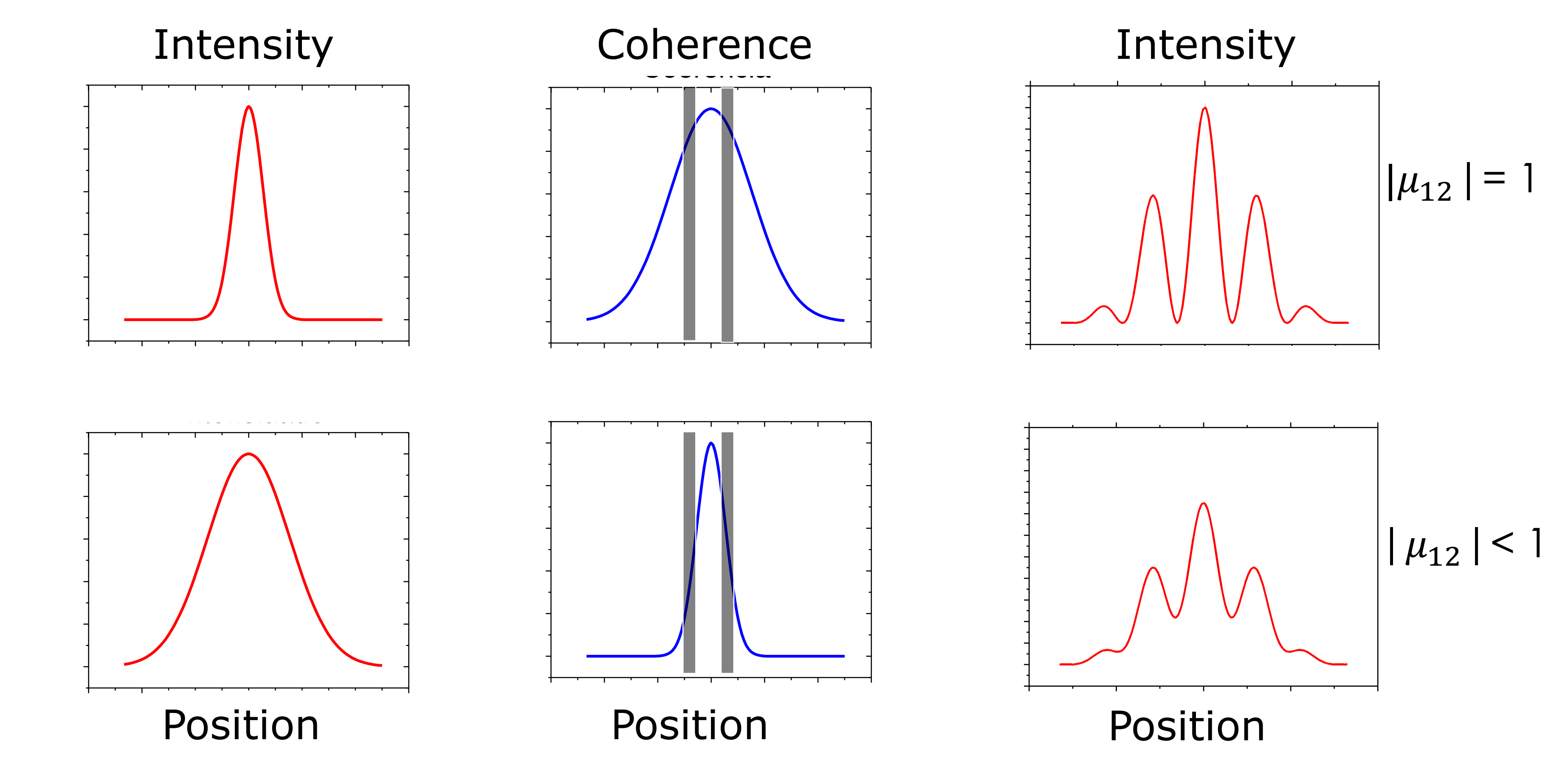

The Gaussian Schell Model (GSM)

THE MULTIPLE PLATE ANTENNA

by

ALLAN CARTER SCHELL

S.B., Massachusetts Institute of Technology
(1956)

S.M., Massachusetts Institute of Technology
(1956)

SUBMITTED IN PARTIAL FULFILLMENT OF THE
REQUIREMENTS FOR THE DEGREE OF
DOCTOR OF SCIENCE
at the
MASSACHUSETTS INSTITUTE OF TECHNOLOGY
September, 1961

THE MULTIPLE PLATE ANTENNA

by

ALLAN CARTER SCHELL

Submitted to the Department of Electrical Engineering on August 21, 1961
in partial fulfillment of the requirements for the degree of Doctor of Science

- 6 -

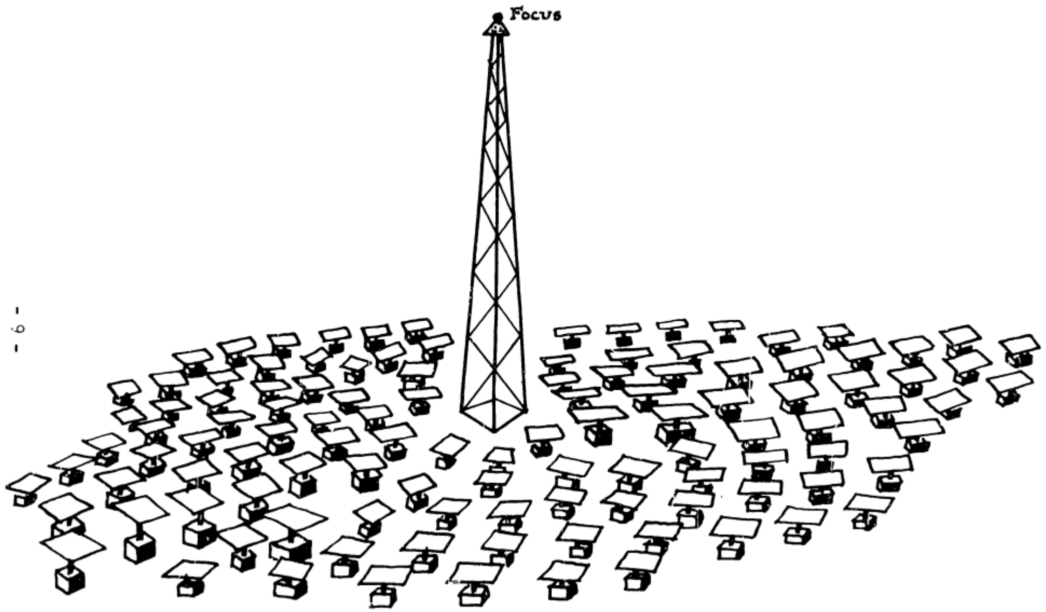

Figure 1

A Sketch of a Multiple Plate Radio Astronomy Antenna

The Gaussian Schell Model (GSM) beams

GAUSSIAN SCHELL-MODEL BEAMS

Ronald J. Sudol

Department of Physics and Astronomy
University of Rochester, Rochester, N.Y. 14627, USA

Ari T. Friberg

Department of Technical Physics
Helsinki University of Technology
SF-02150 Espoo 15, Finland

Leonard Mandel · Emil Wolf *Editors*

Coherence and Quantum Optics V

Proceedings of the Fifth Rochester Conference on Coherence and Quantum Optics held at the University of Rochester, June 13–15, 1983

The Gaussian Schell Model (GSM) beams

In the Schell-model approximation the source cross-spectral density function takes the form

$$W(\underline{\rho}_1,0;\underline{\rho}_2,0) = [I(\underline{\rho}_1,0)I(\underline{\rho}_2,0)]^{\frac{1}{2}}\,\mu(\underline{\rho}_1-\underline{\rho}_2;0)$$

GAUSSIAN SCHELL-MODEL BEAMS

Ronald J. Sudol

Department of Physics and Astronomy
University of Rochester, Rochester, N.Y. 14627, USA

Ari T. Friberg

Department of Technical Physics
Helsinki University of Technology
SF-02150 Espoo 15, Finland

$$I(\underline{\rho},0) = A\exp\{-\rho^2/2\sigma_I^2\}$$

$$\mu(\underline{\rho}';0) = \exp\{-\rho'^2/2\sigma_\mu^2\}$$

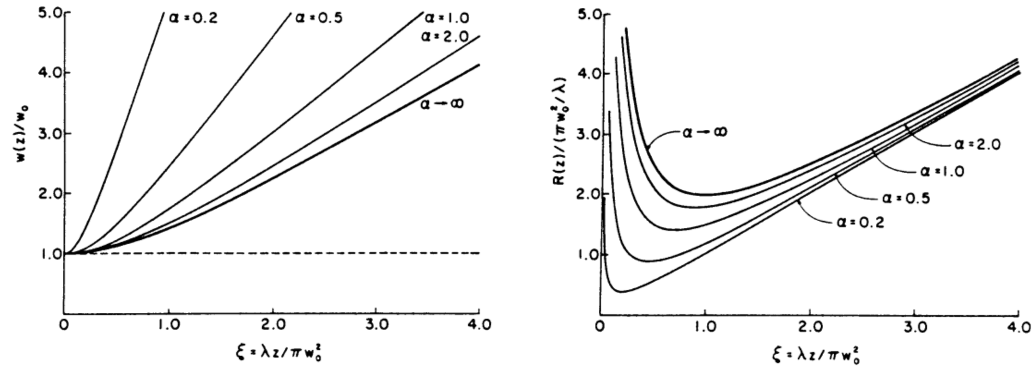

Fig. 1. The behavior of the beam radius w(z) and the radius of curvature R(z) of a Gaussian Schell-model beam as a function of the dimensionless variable $\xi = \lambda\pi/\pi w_0^2$ for several values of the parameter $\alpha = \sigma_\mu/2\sigma_I$. The region $\alpha \ll 1$ correspond to globally incoherent beams (Gaussian quasi-homogeneous beams), whereas the limit $\alpha\to\infty$ represents a fully coherent Gaussian laser beam.

The Gaussian Schell Model (GSM) beams

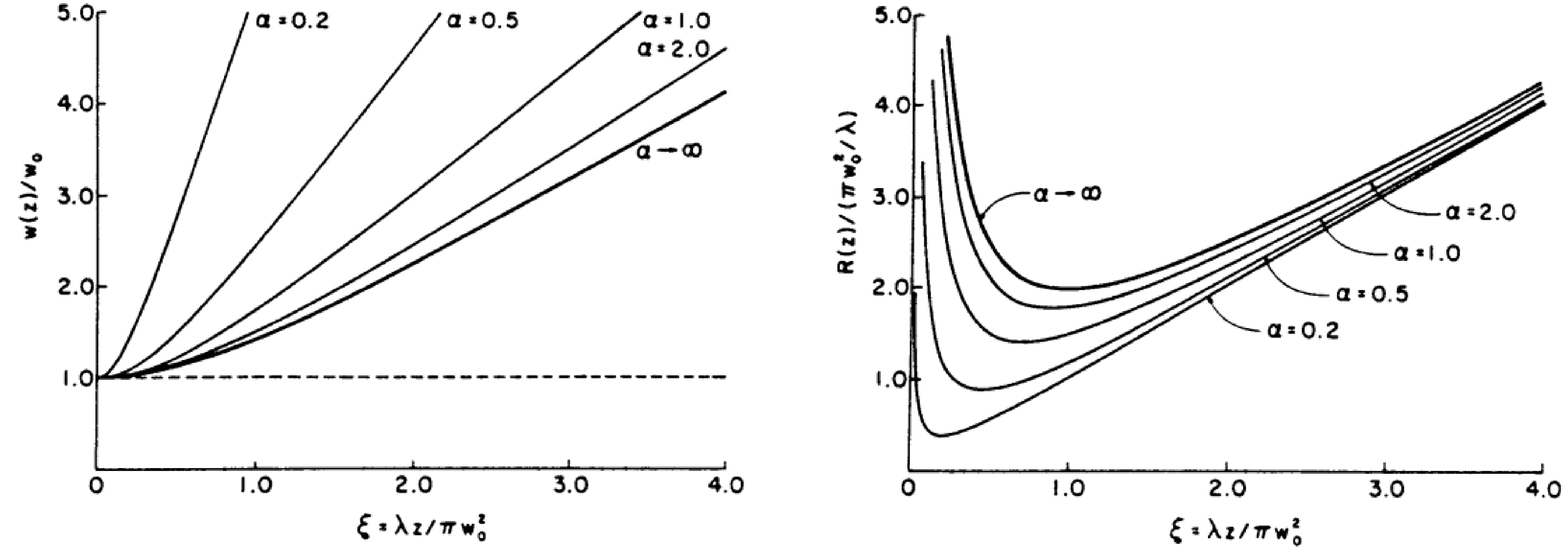

Fig. 1. The behavior of the beam radius w(z) and the radius of curvature R(z) of a Gaussian Schell-model beam as a function of the dimensionless variable $\xi = \lambda\pi / \pi w_0^2$ for several values of the parameter $\alpha = \sigma_\mu / 2\sigma_I$. The region $\alpha << 1$ correspond to globally incoherent beams (Gaussian quasi-homogeneous beams), whereas the limit $\alpha \to \infty$ represents a fully coherent Gaussian laser beam.

The Twisted Gaussian Schell Model (TGSM) beams

R. Simon and N. Mukunda

Vol. 10, No. 1/January 1993/J. Opt. Soc. Am. A 95

Twisted Gaussian Schell-model beams

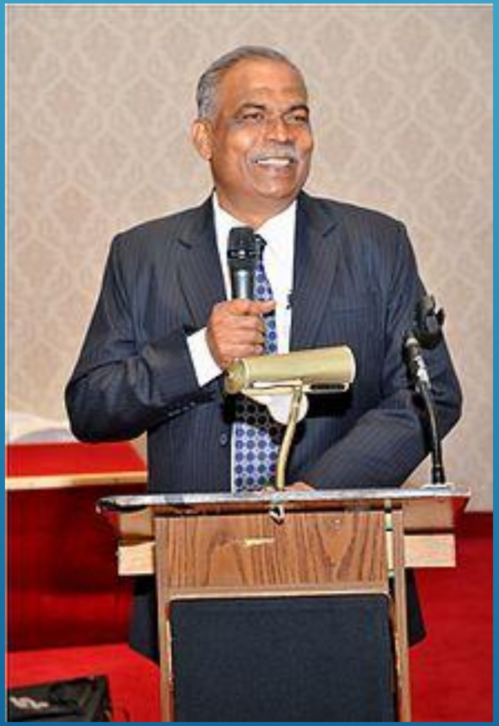

Rajiah Simon

Narasimhaiengar Mukunda

The Twisted Gaussian Schell Model (TGSM) beams

R. Simon and N. Mukunda

Vol. 10, No. 1/January 1993/J. Opt. Soc. Am. A 95

Twisted Gaussian Schell-model beams

We may ask, What is the most general Gaussian cross-spectral density (in a transverse plane) that is invariant under arbitrary rotations about the z axis? The answer

$$\begin{aligned} E(\boldsymbol{\rho}_1, \boldsymbol{\rho}_2) &= a_1({\rho_1}^2 + {\rho_2}^2) + \gamma \boldsymbol{\rho}_1 \cdot \boldsymbol{\rho}_2 \\ &\quad + i a_2({\rho_1}^2 - {\rho_2}^2) + i a_3 \boldsymbol{\rho}_1 \wedge \boldsymbol{\rho}_2 \\ &= (a_1 + \gamma/2)({\rho_1}^2 + {\rho_2}^2) - (\gamma/2)(\boldsymbol{\rho}_1 - \boldsymbol{\rho}_2)^2 \\ &\quad + i a_2({\rho_1}^2 - {\rho_2}^2) + i a_3 \boldsymbol{\rho}_1 \wedge \boldsymbol{\rho}_2 , \end{aligned}$$

$$\boldsymbol{\rho} \wedge \boldsymbol{\rho}' = xy' - yx'$$

$$= \boldsymbol{\rho} \cdot \epsilon \boldsymbol{\rho}'$$

$$\epsilon = i\sigma_2 = \begin{bmatrix} 0 & 1 \\ -1 & 0 \end{bmatrix}$$

The Twisted Gaussian Schell Model (TGSM) beams

R. Simon and N. Mukunda

Vol. 10, No. 1/January 1993/J. Opt. Soc. Am. A 95

Twisted Gaussian Schell-model beams

Using optically defined parameters

$$W_z(\boldsymbol{\rho}_1, \boldsymbol{\rho}_2; \nu) = \frac{I(\nu)}{2\pi\sigma_s(\nu)^2} \times \exp\left[\frac{-1}{4\sigma_s(\nu)^2}(\boldsymbol{\rho}_1{}^2 + \boldsymbol{\rho}_2{}^2) - \frac{(\boldsymbol{\rho}_1 - \boldsymbol{\rho}_2)^2}{2\sigma_g(\nu)^2} \times \frac{-i}{2ƛR(\nu)}(\boldsymbol{\rho}_1{}^2 - \boldsymbol{\rho}_2{}^2) - i\frac{u(\nu)}{ƛ}\boldsymbol{\rho}_1 \cdot \epsilon\boldsymbol{\rho}_2\right]. \quad (2.2)$$

I is the intensity

σ_s is the beam width

σ_g is the coherence length

R is radius of curvature

u is the twist phase parameter

$ƛ = \lambda/2\pi$

The Twisted Gaussian Schell Model (TGSM) beams

Twisted Gaussian Schell-model beams

Effects on divergence

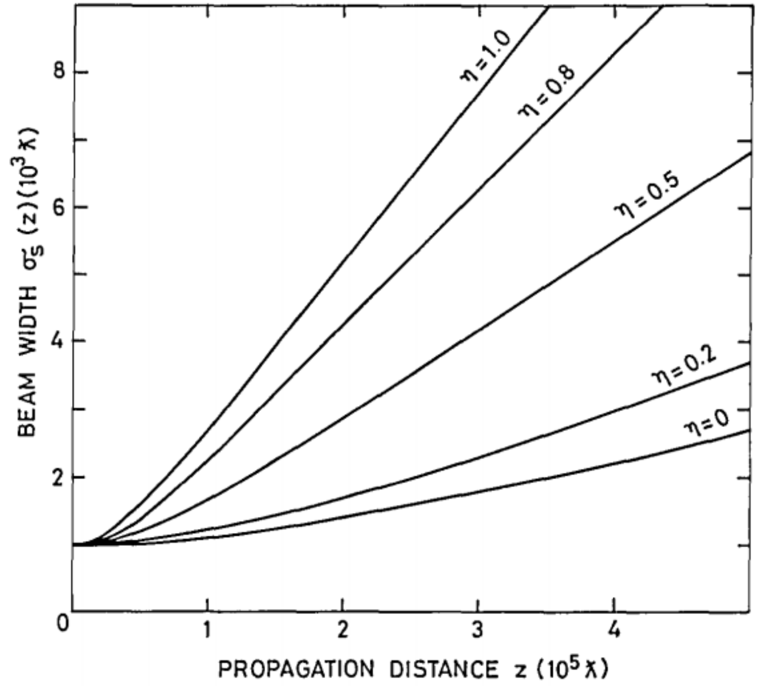

Fig. 1. Effect of the invariant twist phase on beam expansion, with $\beta = 5$, $\sigma_s(0) = 10^3ƛ$.

Effect on the propagation phase

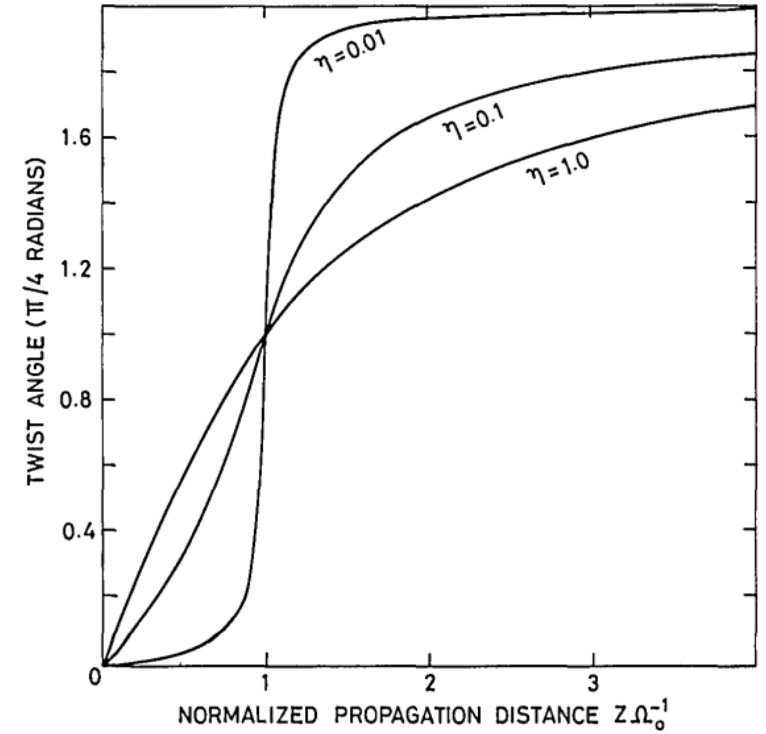

Fig. 2. Twist phenomenon in free propagation, with $\beta = 5$.

$$\beta = \sigma_s(z)/\sigma_g(z) = \sigma_s(0)/\sigma_g(0)$$

$\sigma_g(\nu)$ Cohrerence length

$\sigma_s(\nu)$ Beam width

The Twisted Gaussian Schell Model (TGSM) beams illustrating beam rotation

photonics

Article

Statistical Characteristics of a Twisted Anisotropic Gaussian Schell-Model Beam in Turbulent Ocean

Yonglei Liu [1,2], Yuefeng Zhao [1,2], Xianlong Liu [1,2], Chunhao Liang [1,2], Lin Liu [3], Fei Wang [3] and Yangjian Cai [1,2,3,*]

Photonics **2020**, *7*, 37;

doi:10.3390/photonics7020037

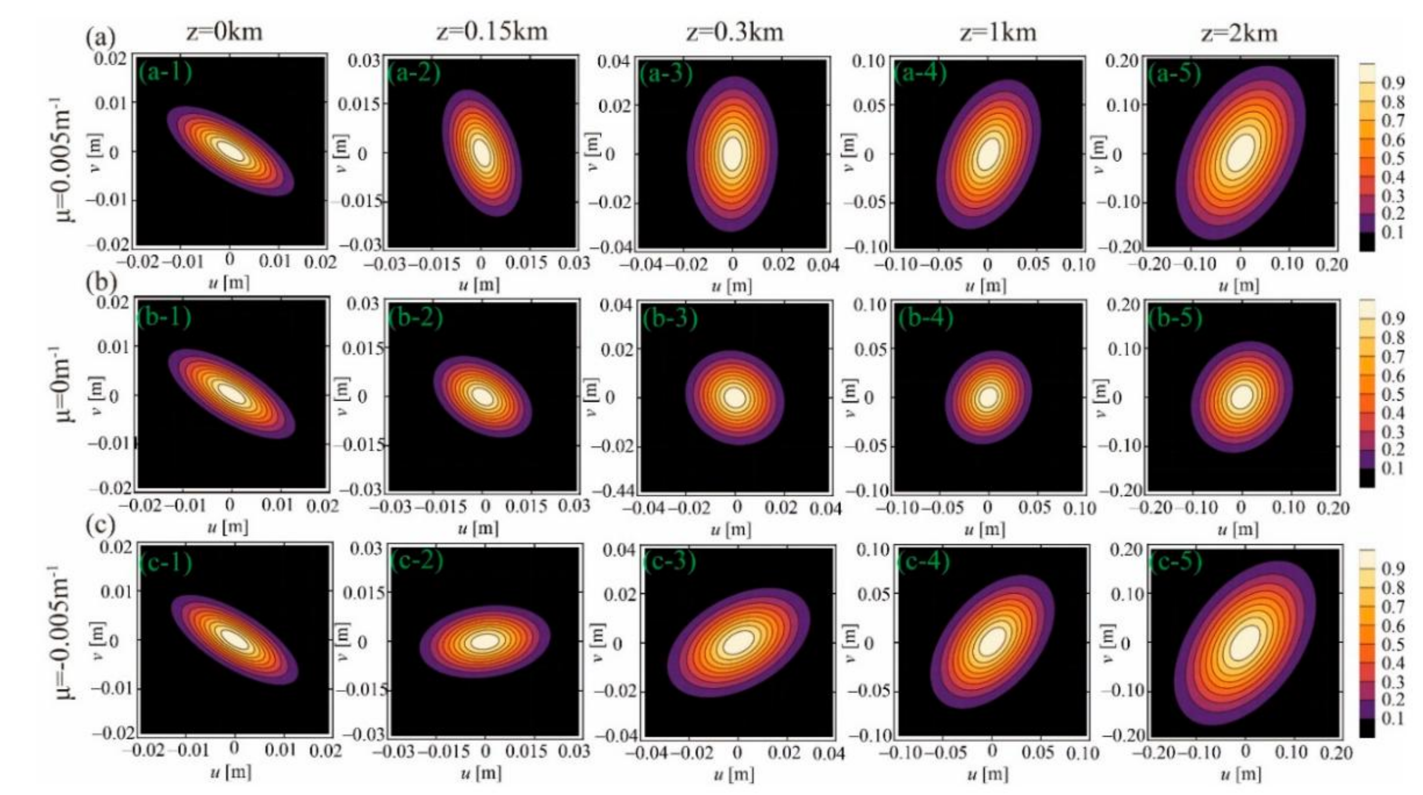

TGSM beams motivation

Classical Optics: Robustness against Propagation in turbulent media

F. Wang and Y. Cai, "Second-order statistics of a twisted Gaussian Schell-model beam in turbulent atmosphere," *Opt. Express*, vol. 18, p. 24661, 2010.

M. Zhou, W. Fan, and G. Wu, "Evolution properties of the orbital angular momentum spectrum of twisted Gaussian Schell-model beams in turbulent atmosphere," *J. Opt. Soc. Am. A*, vol. 37, p. 142, 2020.

Y. Liu, X. Liu, L. Liu, F. Wang, Y. Zhang, and Y. Cai, "Ghost imaging with a partially coherent beam carrying twist phase in a turbulent ocean: a numerical approach," *Appl. Sci.*, vol. 9, 2019, Art no. 3023.

Quantum Optics: Robustness against Propagation in turbulent media

Samukelisiwe Purity Phehlukwayo , Marie Louise Umuhire , Yaseera Ismail, Stuti Joshi , and Francesco Petruccione , Influence of coincidence detection of a biphoton state through free-space atmospheric turbulence using a partially spatially coherent pump, Phys. Rev. A 102, 033732 (2020)

Quantum Optics: Boosting quantum entanglement

L. Hutter, G. Lima, and S. P. Walborn, "Boosting entanglement generation in down-conversion with incoherent illumination," *Phys. Rev. Lett.*, vol. 125, p. 193602, 2020.

TGSM beams: generation

1818 J. Opt. Soc. Am. A/Vol. 11, No. 6/June 1994

Interpretation and experimental demonstration of twisted Gaussian Schell-model beams

Ari T. Friberg, Eero Tervonen, and Jari Turunen

Department of Technical Physics, Helsinki University of Technology, FIN- 02150 Espoo, Finland

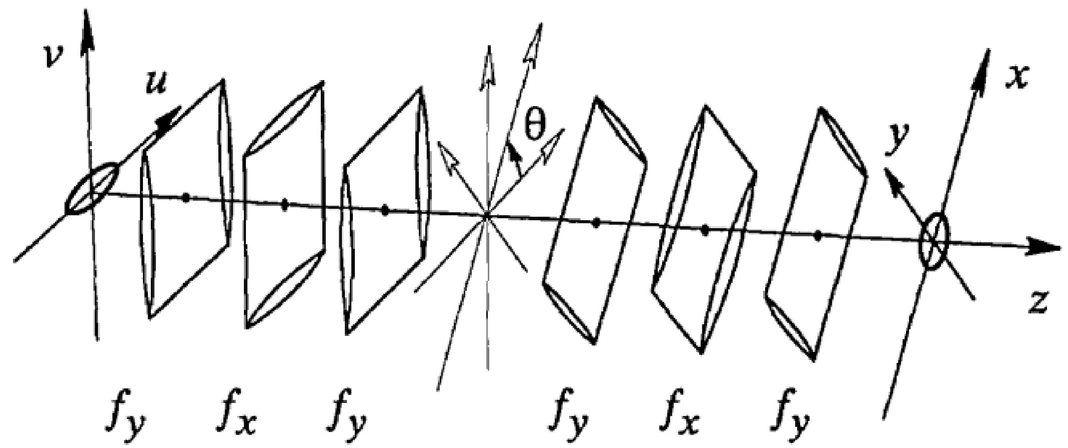

Fig. 1. Astigmatic optical lens system used for converting an anisotropic GSM beam into a twisted GSM beam.

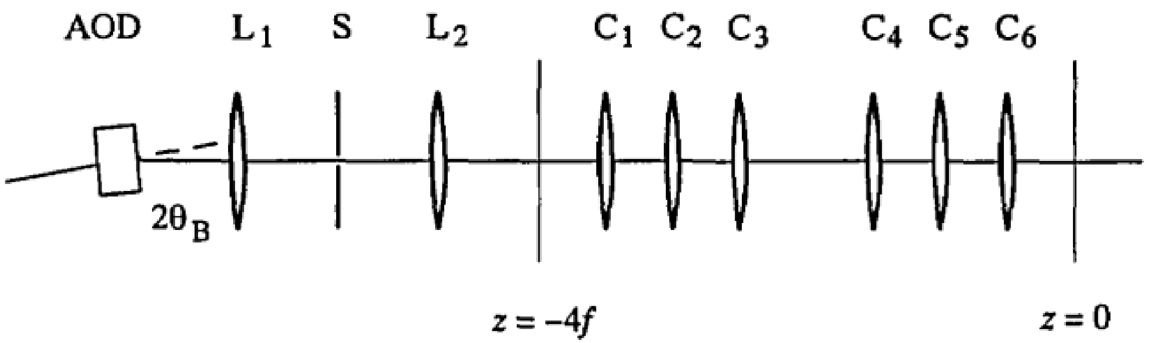

Fig. 5. Experimental arrangement: AOD, acousto-optic deflector; L_1 and L_2, spherical lenses; $C_1 - C_6$, cylindrical lenses; S, spatial filter.

TGSM beams: generation

Letter Vol. 44, No. 15 / 1 August 2019 / *Optics Letters* 3709

Optics Letters

Generating bona fide twisted Gaussian Schell-model beams

Haiyun Wang,[1] Xiaofeng Peng,[1] Lin Liu,[1,5] Fei Wang,[1,6] Yangjian Cai,[1,2,7] and Sergey A. Ponomarenko[3,4]

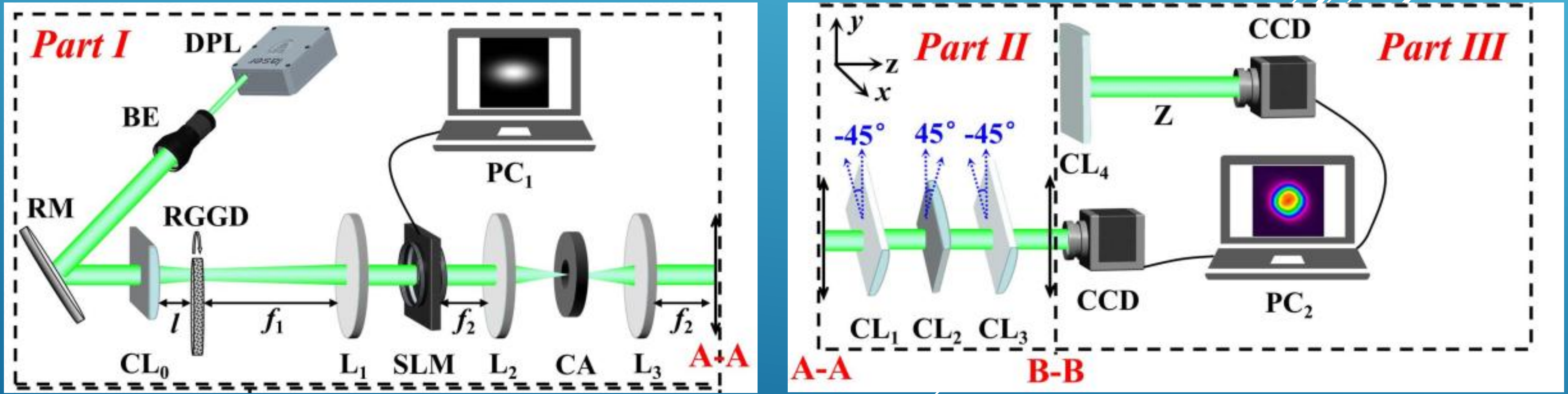

Fig. 1. Experimental setup for generating a TGSM beam. DPSS, diode-pumped solid-state laser; BE, beam expander; RM, reflecting mirror; CL_0, CL_1, CL_2, CL_3, and CL_4, thin cylindrical lenses; RGGD, rotating ground glass disk; L_1, L_2, and L_3, thin lenses; SLM, spatial light modulator; CA, circular aperture; CCD, charge-coupled device; PC_1 and PC_2, personal computers.

TGSM beams: generation

Research Article Vol. 29, No. 25 / 6 Dec 2021 / *Optics Express* 41964

Optics EXPRESS

Generating a twisted Gaussian Schell-model beam with a coherent-mode superposition

YUE ZHANG,[1] XUAN ZHANG,[1] HAIYUN WANG,[1] YAN YE,[2] LIN LIU,[1,4] YAHONG CHEN,[1,5] FEI WANG,[1,6] AND YANGJIAN CAI[1,3,7]

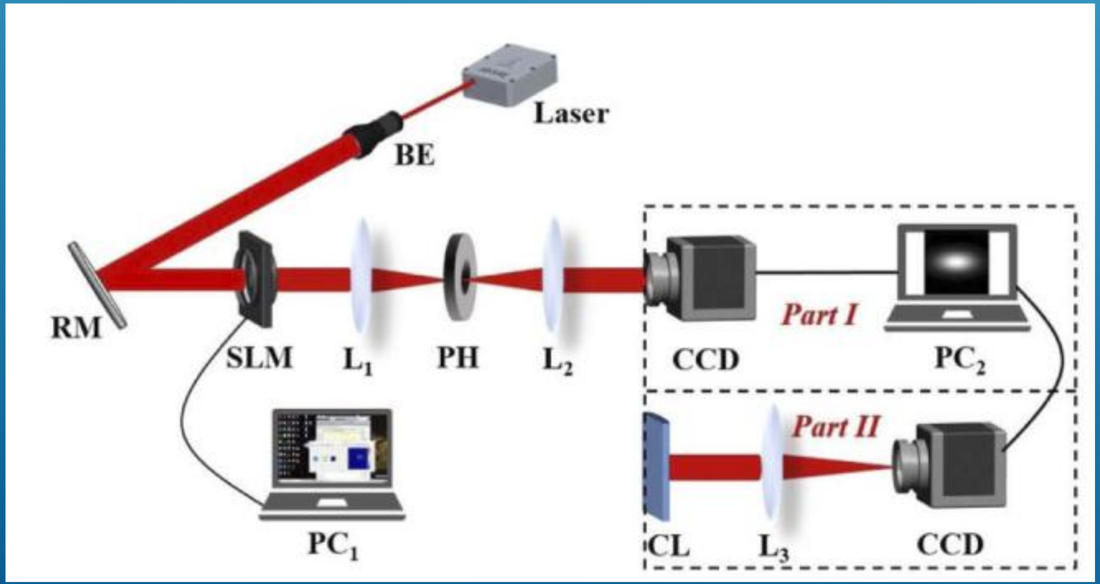

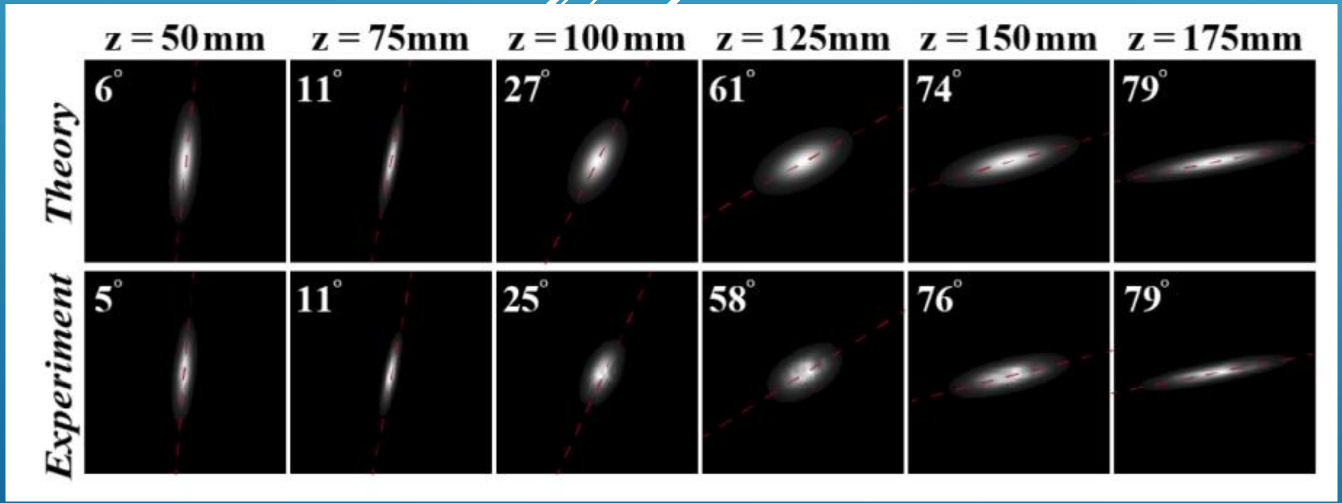

TGSM beams: generation

DE GRUYTER

Nanophotonics 2022; 11(4): 689–696

Research Article

Haiyun Wang, Xiaofeng Peng, Hao Zhang, Lin Liu*, Yahong Chen*, Fei Wang* and Yangjian Cai*

Experimental synthesis of partially coherent beam with controllable twist phase and measuring its orbital angular momentum

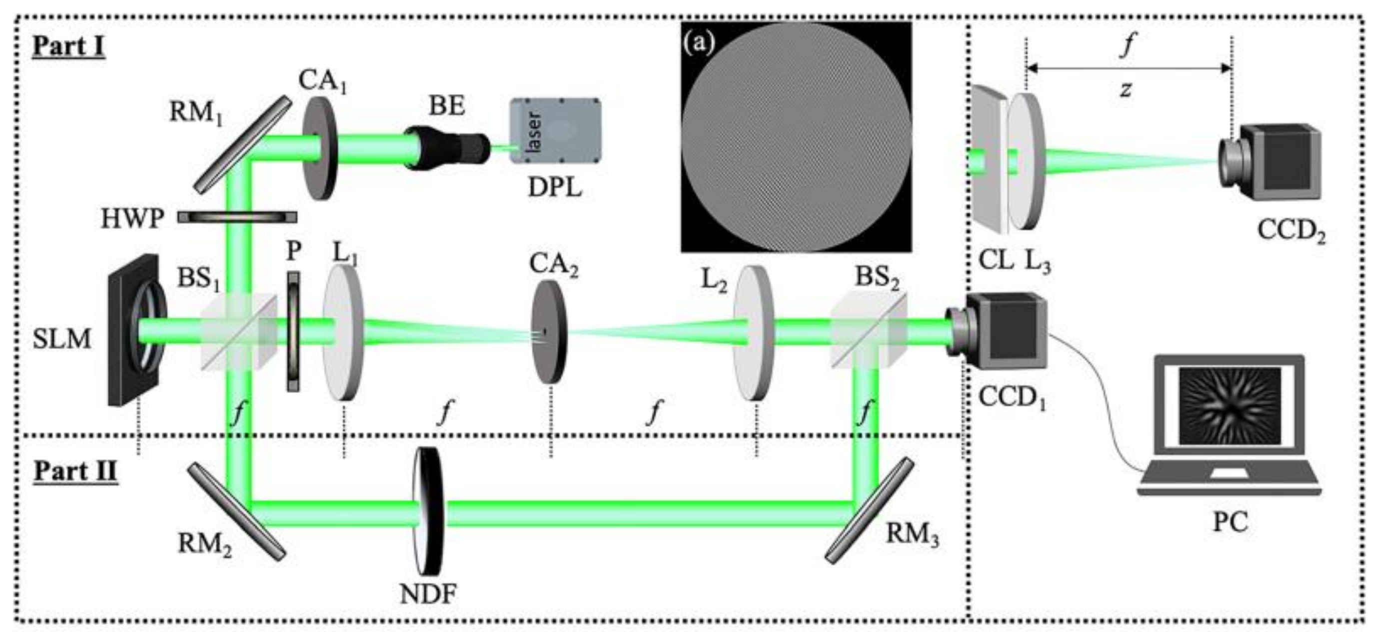

TGSM beams: generation

DE GRUYTER Nanophotonics 2022; 11(4): 689–696

Research Article

Haiyun Wang, Xiaofeng Peng, Hao Zhang, Lin Liu*, Yahong Chen*, Fei Wang* and Yangjian Cai*

Experimental synthesis of partially coherent beam with controllable twist phase and measuring its orbital angular momentum

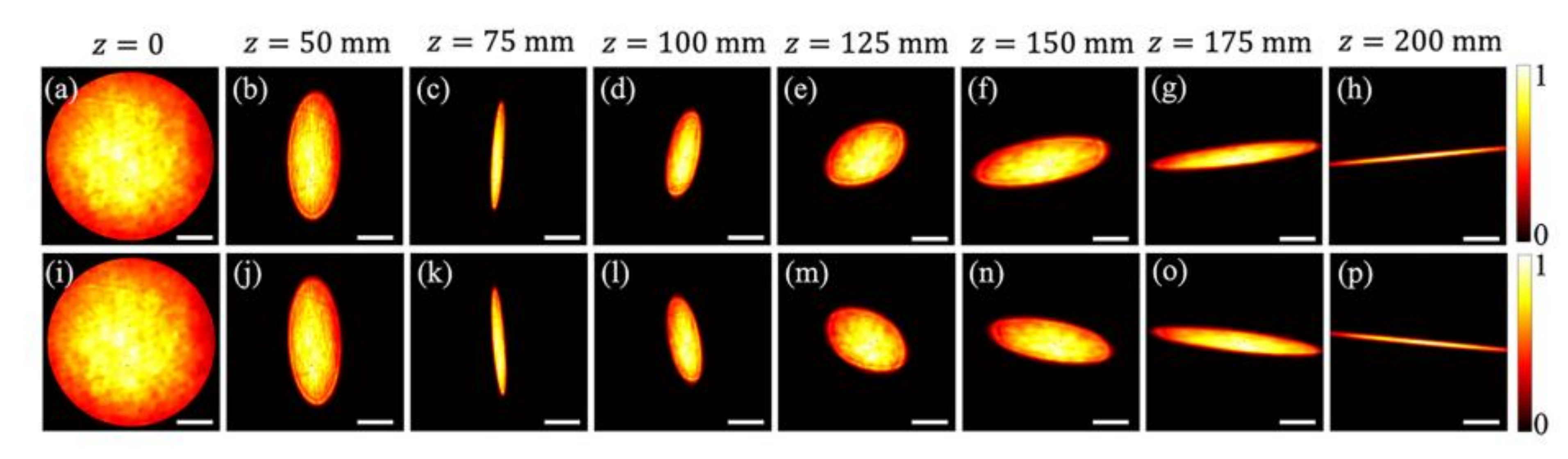

SLM movie method for generating TGSM beams

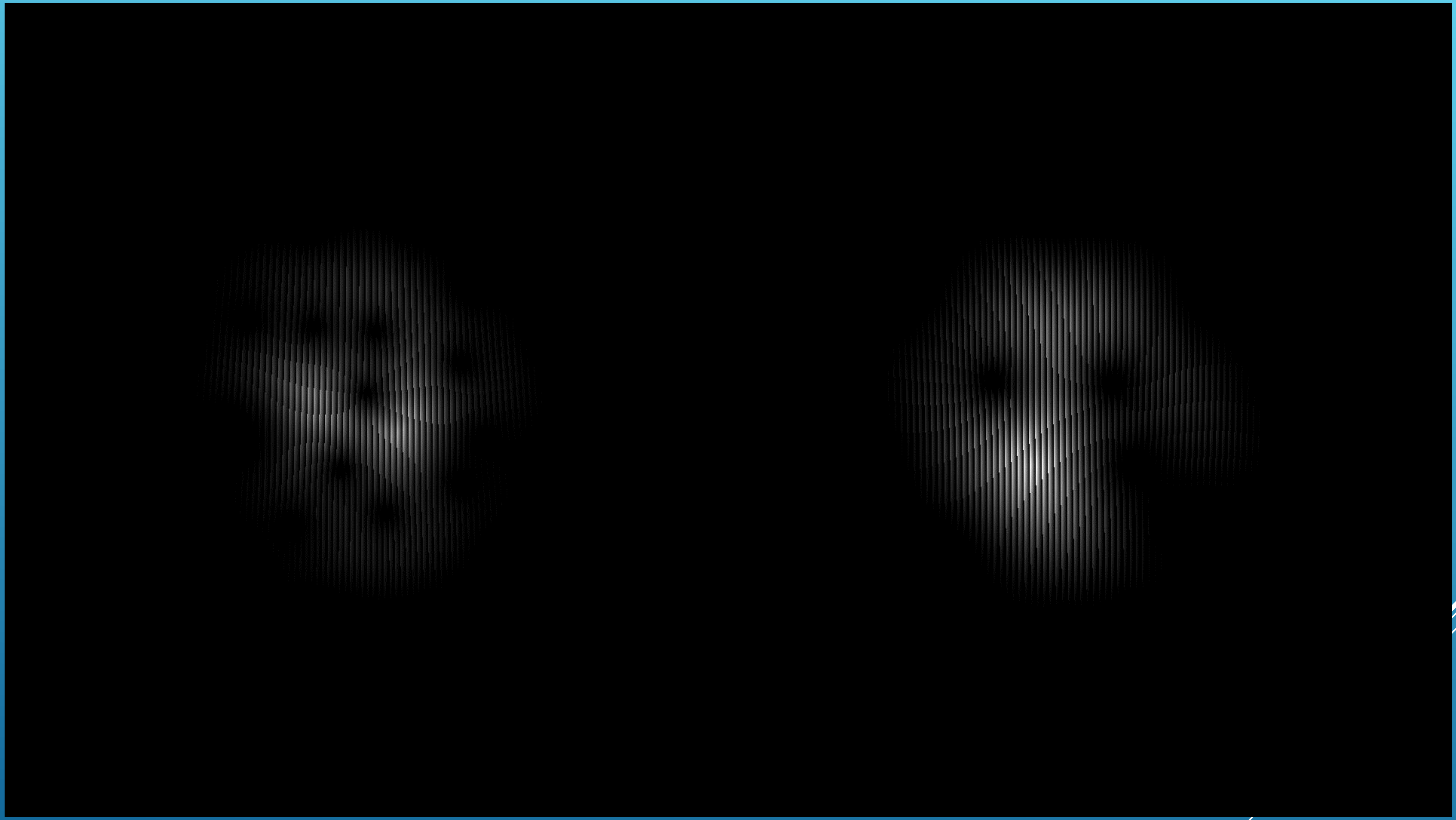

Parametric Down-conversion

Spontenous emission (SPDC)

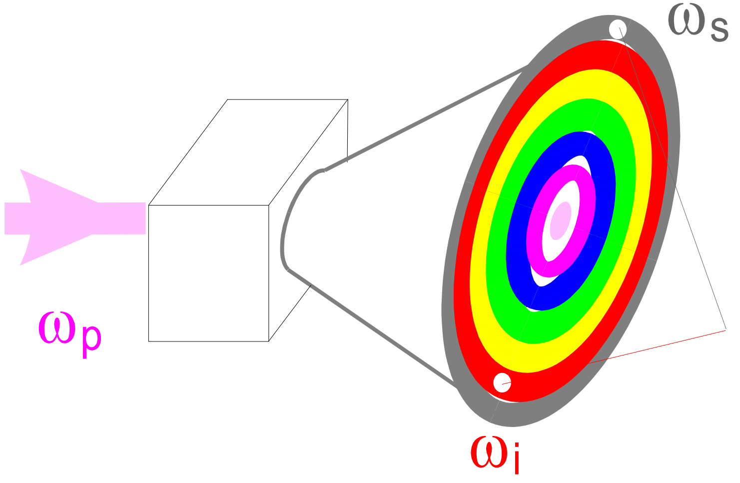

$$\hbar\omega_p = \hbar\omega_i + \hbar\omega_s$$

$$\vec{k}_p = \vec{k}_i + \vec{k}_s$$

Stimulated emission (StimPDC)

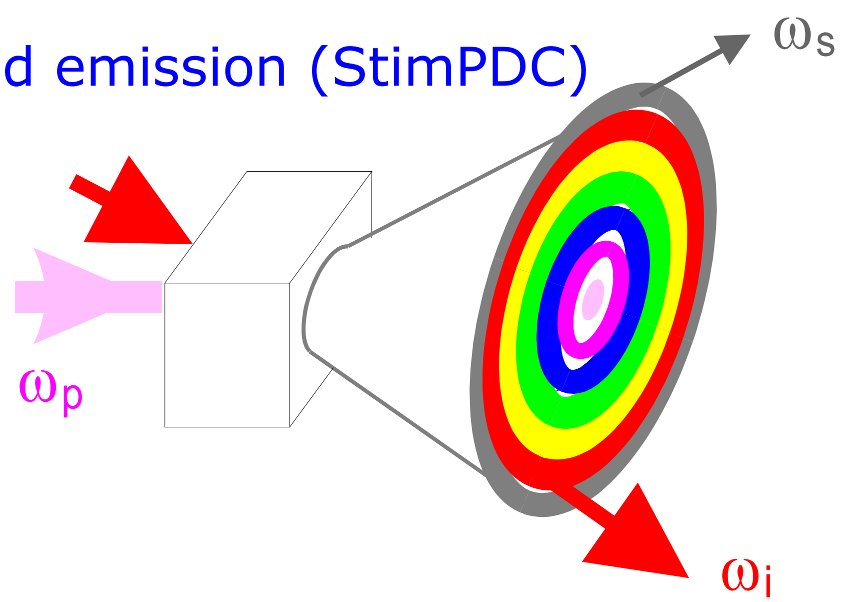

Spatial Entanglement Can Be Measured And Witnessed

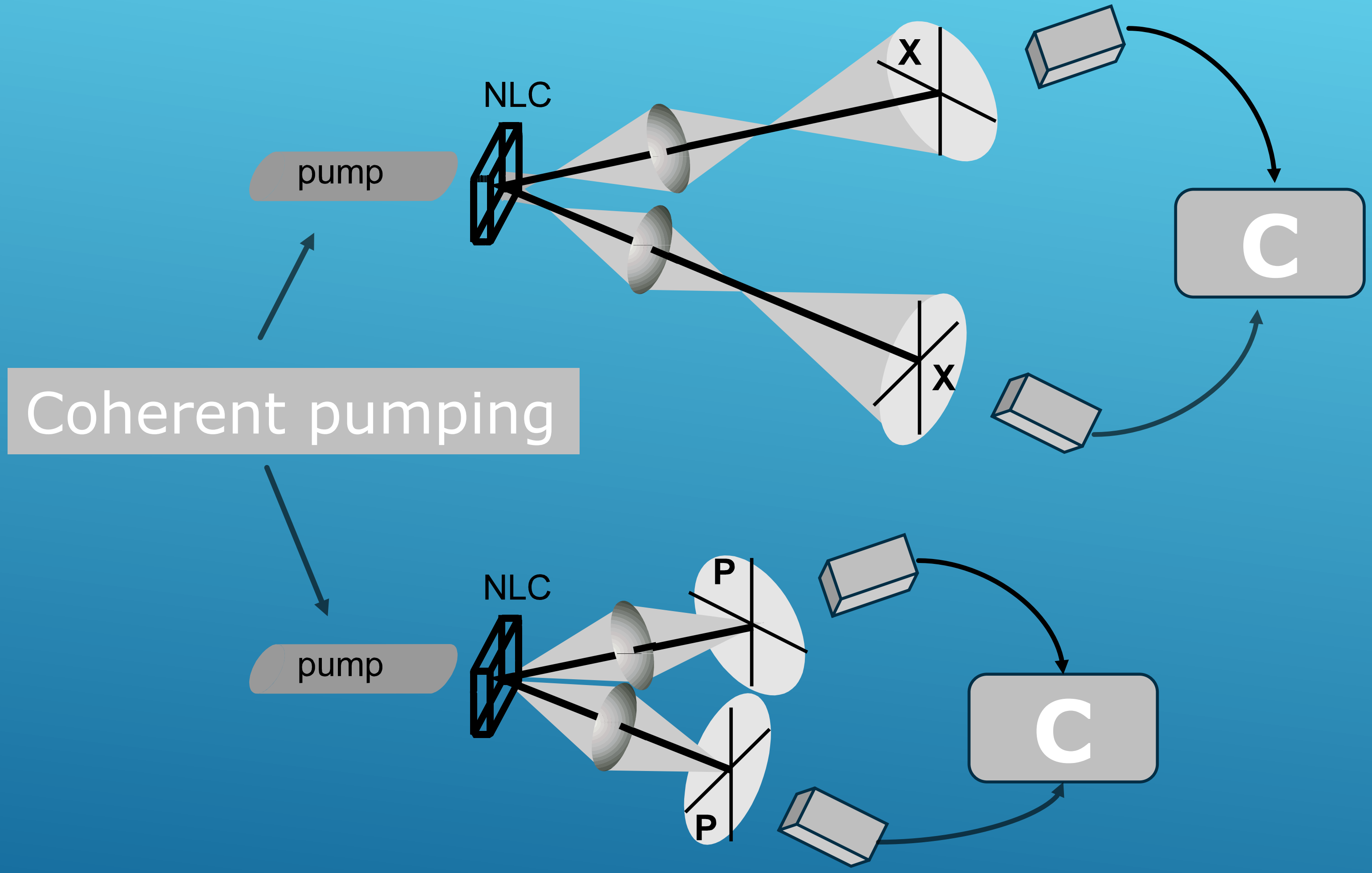

Spatial Entanglement Can Be Witnessed

Lu-Ming Duan, G. Giedke, J. I. Cirac, and P. Zoller
Phys. Rev. Lett. 84, 2722 (2000).

DGCZ criterion

$$(\Delta(x_1 - x_2))^2 + (\Delta(p_1 + p_2))^2 < 2$$

MGVT criterion

S. Mancini, V. Giovannetti, D. Vitali, and P. Tombesi
Phys. Rev. Lett. 88, 120401 (2002).

$$(\Delta(x_1 - x_2))^2 (\Delta(p_1 + p_2))^2 < 1$$

Spatial Entanglement Can Be Measured And Witnessed

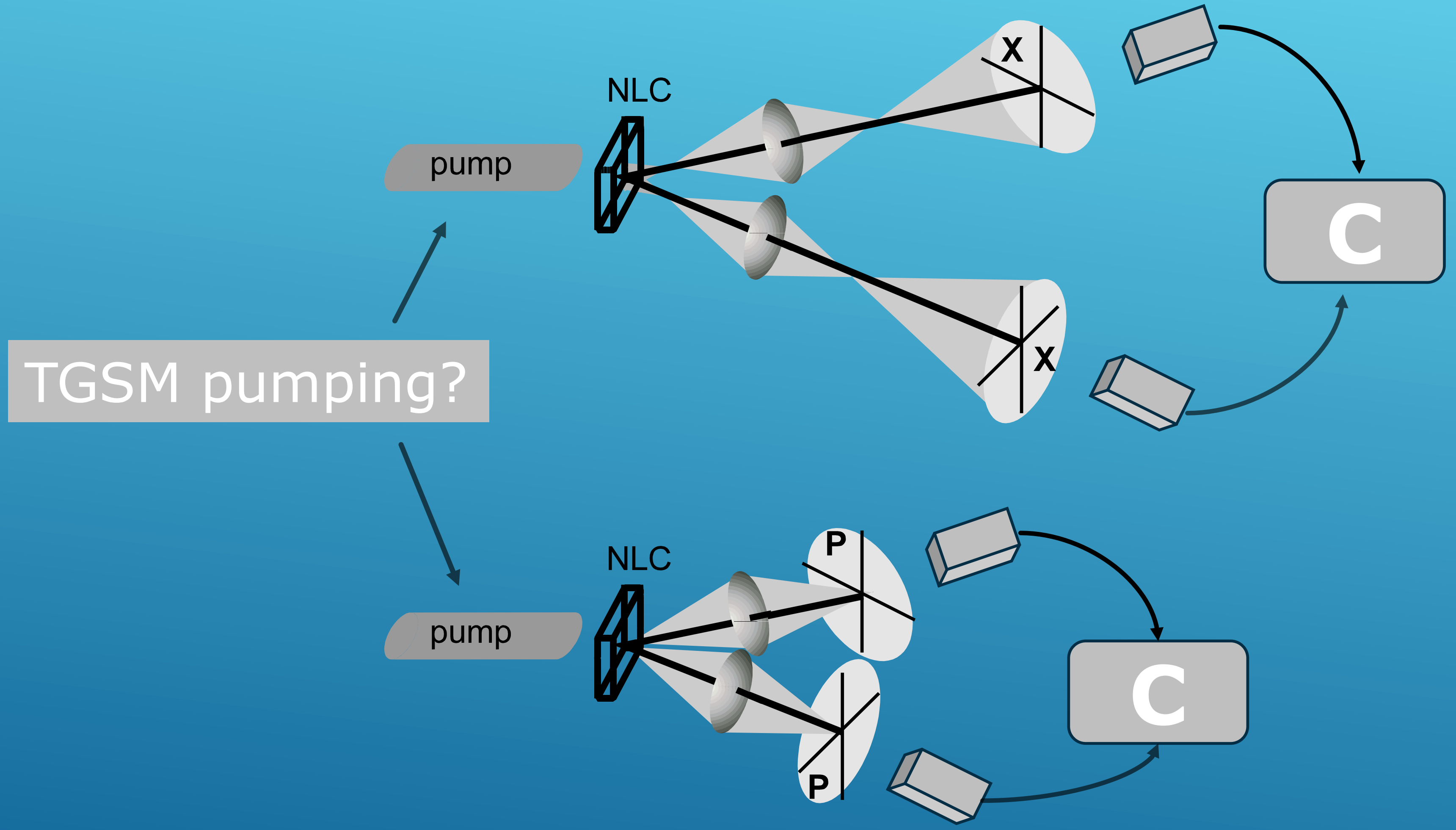

Incoherence degrades spatial correlations

PHYSICAL REVIEW A **99**, 053831 (2019)

Spatially entangled photon-pair generation using a partial spatially coherent pump beam

Hugo Defienne* and Sylvain Gigan

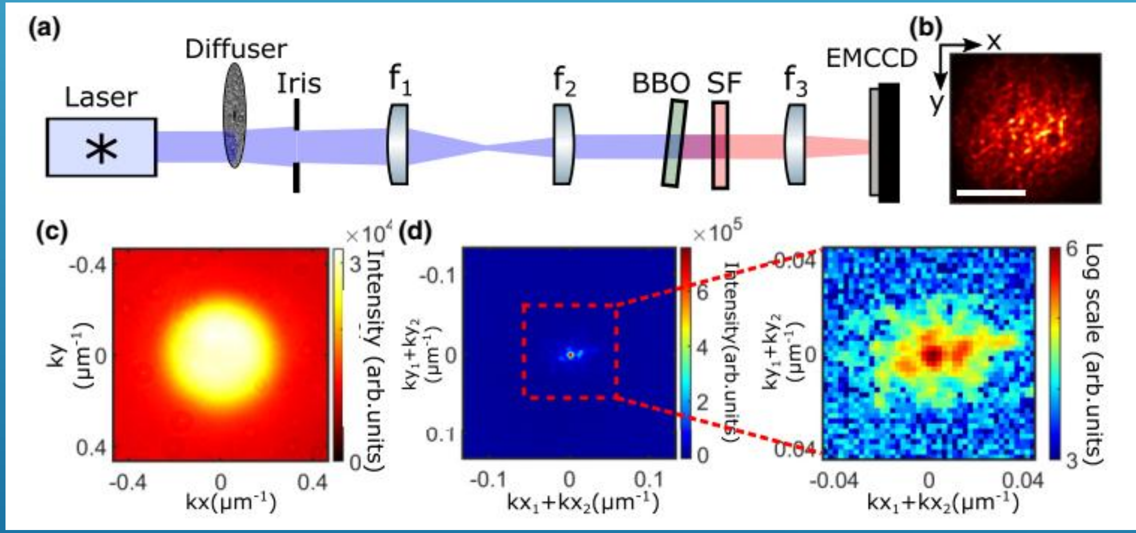

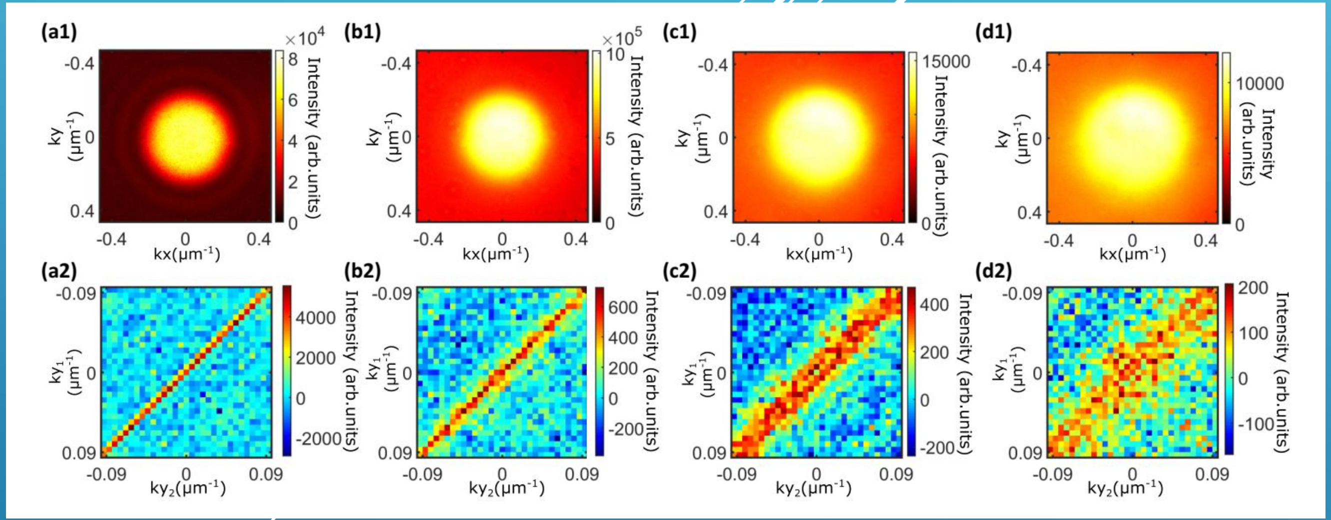

Pumping SPDC with partially coherent pump

PHYSICAL REVIEW A **102**, 033732 (2020)

Influence of coincidence detection of a biphoton state through free-space atmospheric turbulence using a partially spatially coherent pump

Samukelisiwe Purity Phehlukwayo,[1] Marie Louise Umuhire,[1] Yaseera Ismail,[1,*] Stuti Joshi,[2,†] and Francesco Petruccione[1,3,‡]

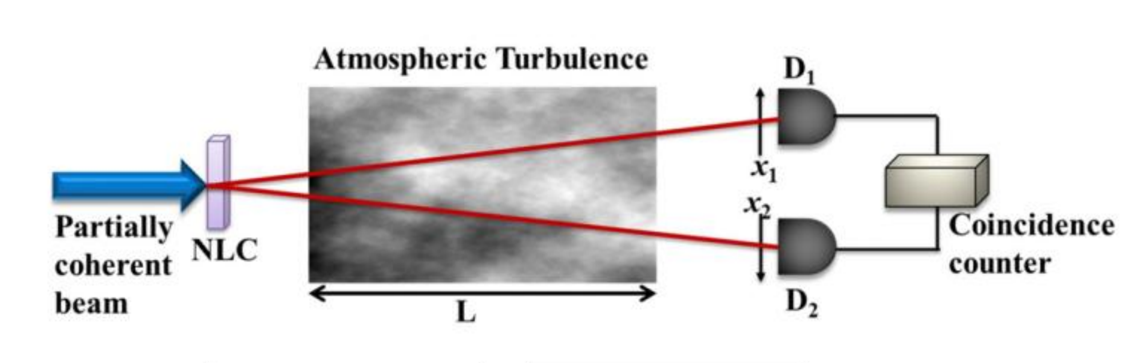

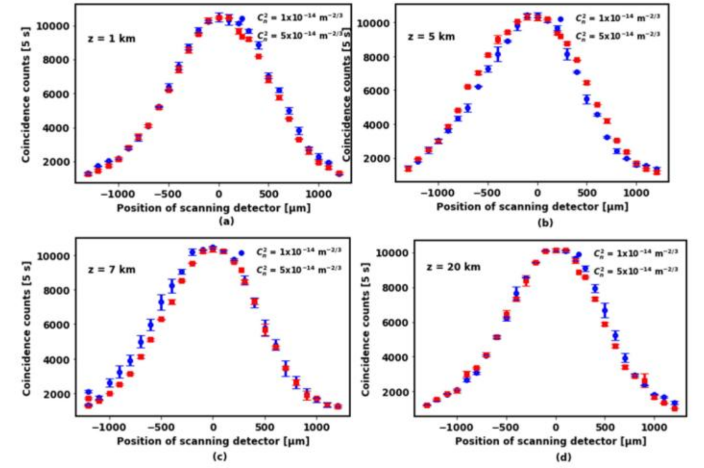

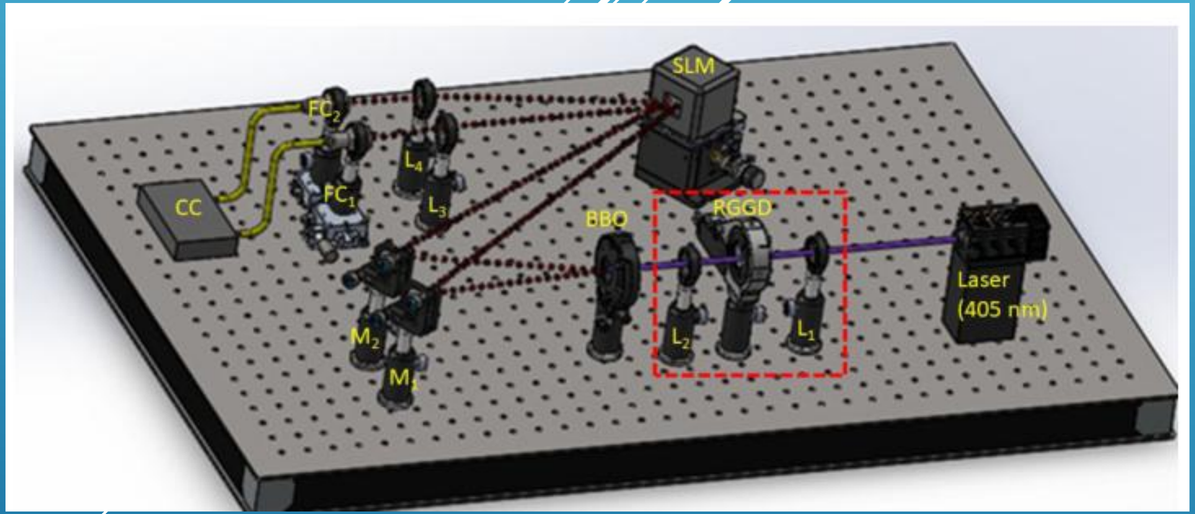

Incoherence degrades spatial correlations

Research Article
Vol. 27, No. 15 | 22 Jul 2019 | OPTICS EXPRESS 20745
Optics EXPRESS

Influence of pump coherence on the generation of position-momentum entanglement in optical parametric down-conversion

WUHONG ZHANG,[1,2] ROBERT FICKLER,[2,3] ENNO GIESE,[2,4,6] LIXIANG CHEN,[1,7] AND ROBERT W. BOYD[2,5]

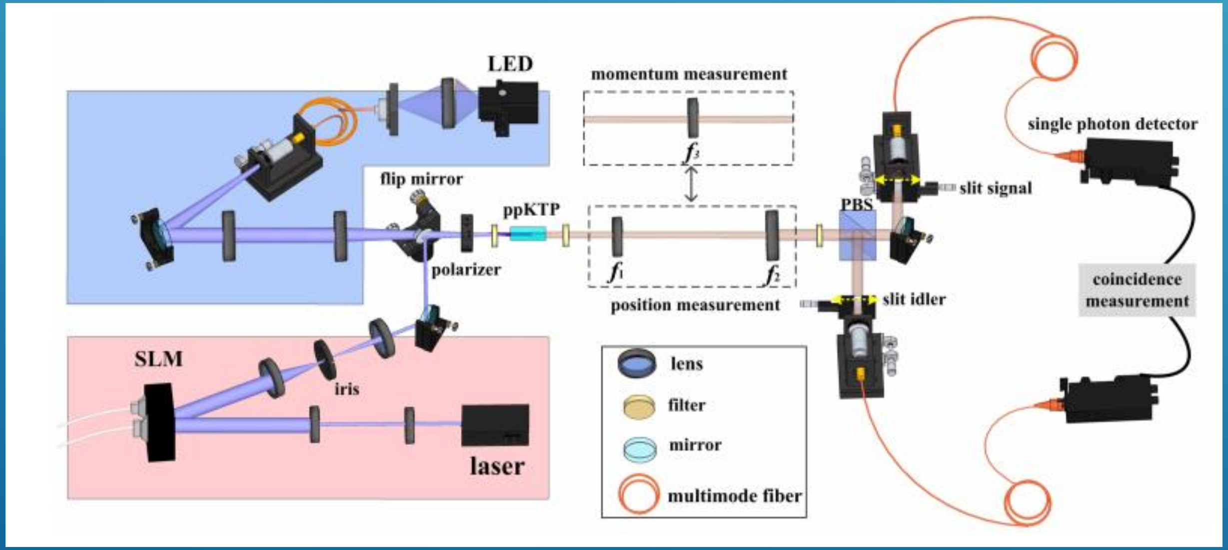

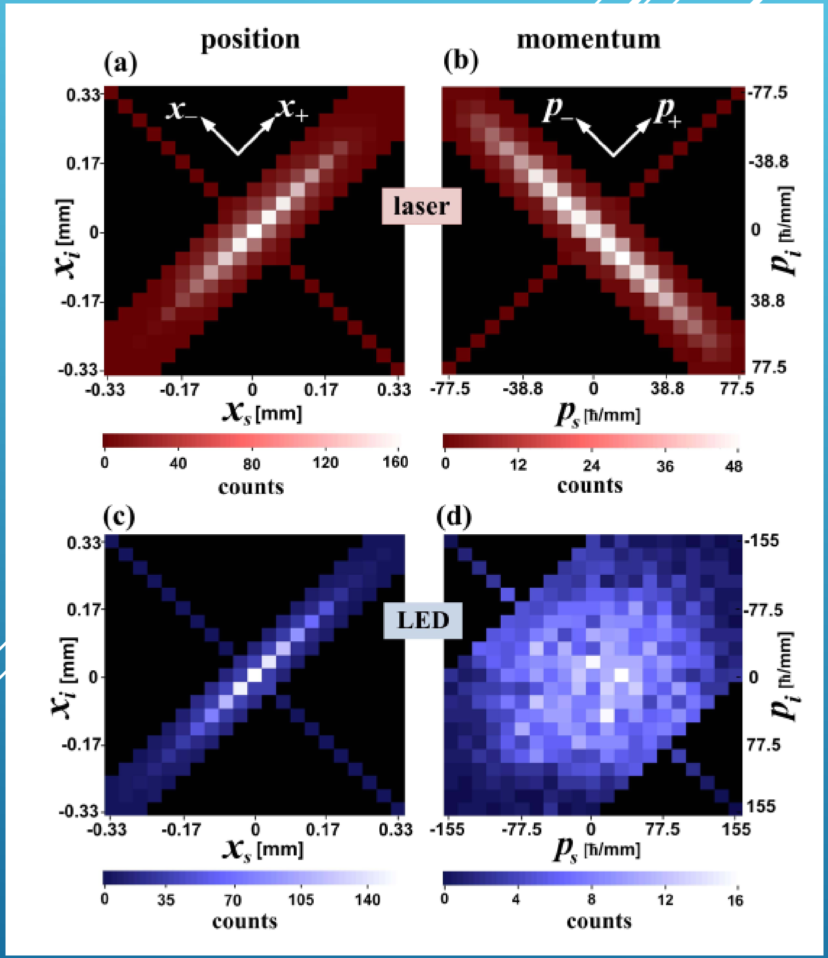

TGSM beam pumping can increase entanglement!

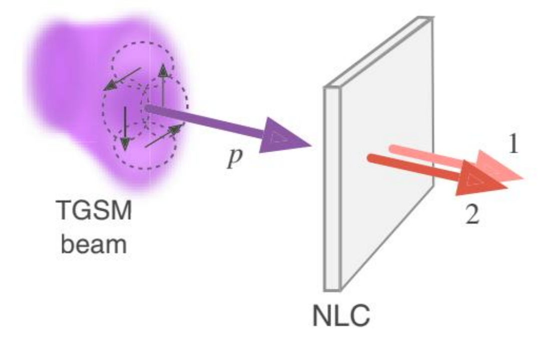

PHYSICAL REVIEW LETTERS **125**, 193602 (2020)

Boosting Entanglement Generation in Down-Conversion with Incoherent Illumination

Lucas Hutter[1,2] G. Lima,[3,4] and S. P. Walborn[1,3,4]

A TGSM beam is therefore uniquely characterized by its CM [23,24]:

$$T = \begin{pmatrix} \sigma^2 & -\frac{k\sigma^2}{R} & 0 & ku\sigma^2 \\ -\frac{k\sigma^2}{R} & \tau^2 & -ku\sigma^2 & 0 \\ 0 & -ku\sigma^2 & \sigma^2 & -\frac{k\sigma^2}{R} \\ ku\sigma^2 & 0 & -\frac{k\sigma^2}{R} & \tau^2 \end{pmatrix}. \quad (1)$$

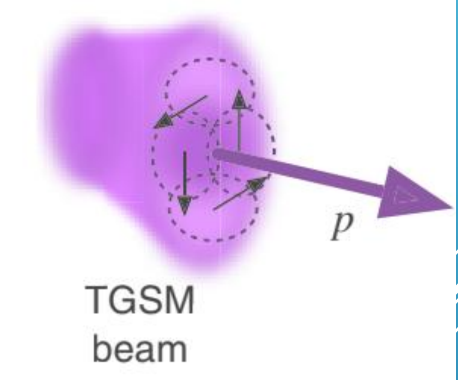

σ is the beam waist

$\tau^2 = (1/\delta^2) + (1/4\sigma^2) + k^2[(\sigma^2/R^2) + u^2\sigma^2)]$

is the variance of the wave vector distribution.

δ is the transverse coherence length.

R is the radius of curvature

u is the so-called twist phase

k is the wave number

TGSM beam pumping can increase entanglement!

Two-photon covariance matrix

$$V_{12} = \begin{pmatrix} A & C \\ C^T & B \end{pmatrix}, \quad (4)$$

A (B) refer to photon 1 (2)

$A = B$

$$A = \begin{pmatrix} \sigma^2 + \sigma_-^2 & -\frac{k\sigma^2}{2R} & 0 & \frac{ku\sigma^2}{2} \\ -\frac{k\sigma^2}{2R} & \frac{1}{4}(\tau^2 + \Delta_-^2) & -\frac{ku\sigma^2}{2} & 0 \\ 0 & -\frac{ku\sigma^2}{2} & \sigma^2 + \sigma_-^2 & -\frac{k\sigma^2}{2R} \\ \frac{ku\sigma^2}{2} & 0 & -\frac{k\sigma^2}{2R} & \frac{1}{4}(\tau^2 + \Delta_-^2) \end{pmatrix}$$

$\sigma_-^2 = 9L/10k$

L is the length of the crystal

$\Delta_-^2 = 3k/2L$

$$C = \begin{pmatrix} \sigma^2 - \sigma_-^2 & -\frac{k\sigma^2}{2R} & 0 & \frac{ku\sigma^2}{2} \\ -\frac{k\sigma^2}{2R} & \frac{1}{4}(\tau^2 - \Delta_-^2) & -\frac{ku\sigma^2}{2} & 0 \\ 0 & -\frac{ku\sigma^2}{2} & \sigma^2 - \sigma_-^2 & -\frac{k\sigma^2}{2R} \\ \frac{ku\sigma^2}{2} & 0 & -\frac{k\sigma^2}{2R} & \frac{1}{4}(\tau^2 - \Delta_-^2) \end{pmatrix}$$

The symplectic eigenvalues of Eq. (4) are twofold degenerate and given by [37]

$$\lambda_{\pm} = \frac{1}{\sqrt{2}} \left| \sqrt{a_{+} \pm \sqrt{4k^2 \Delta_{-}^2 \sigma_{-}^2 \sigma^4 \left(u^2 + \frac{1}{R^2} \right) + a_{-}^2}} \right|, \qquad (8)$$

where $a_{\pm} = \tau^2 \sigma_{-}^2 \pm \Delta_{-}^2 \sigma^2$.

Entanglement is confirmed when $\lambda_{-} < 1/2$ (gray horizontal plane). The SPDC parameters are $R = \infty$, $\lambda_p = 400$ nm, $\sigma_p = 50$ μm, and $L = 1$ cm. (b) Profile plots of λ_{-} for normalized twist phase $|u|/k\delta^2$ equal to zero (black solid line), 1 (red solid line), and 1/2 (blue dashed line). The dotted black curve is the near-field and far-field entanglement criteria (7).

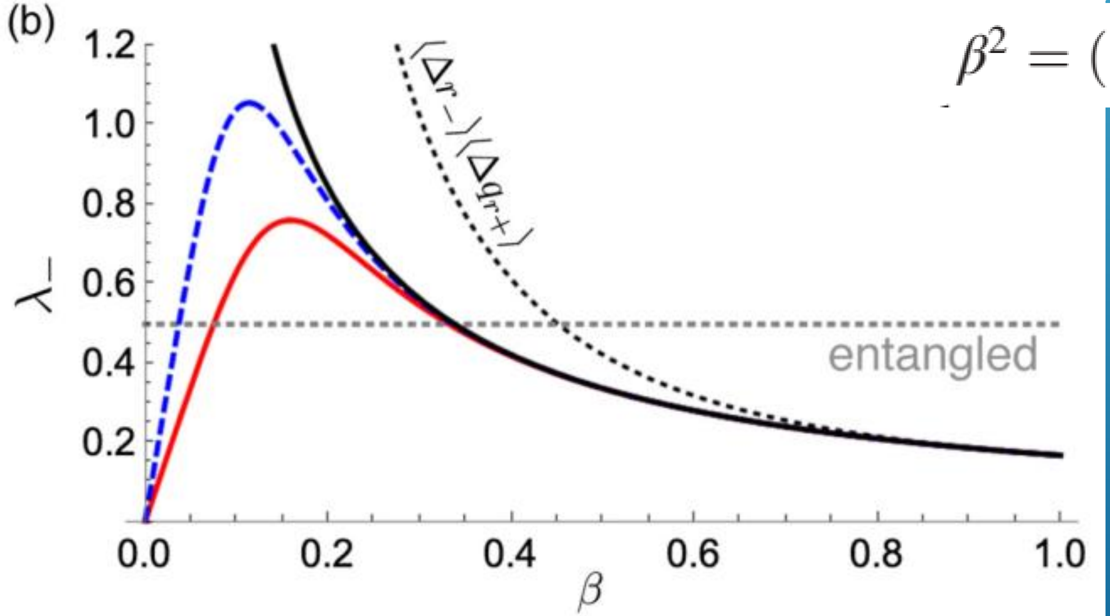

$$\beta^2 = (1 + 4\sigma^2/\delta^2)^{-1}$$

DE GRUYTER Nanophotonics 2022; 11(4): 763–770

Research Article

Gustavo H. dos Santos, Andre G. de Oliveira, Nara Rubiano da Silva, Gustavo Cañas, Esteban S. Gómez, Stuti Joshi, Yaseera Ismail, Paulo H. Souto Ribeiro and Stephen Patrick Walborn*

Phase conjugation of twisted Gaussian Schell model beams in stimulated down-conversion

Stimulated emission (StimPDC)

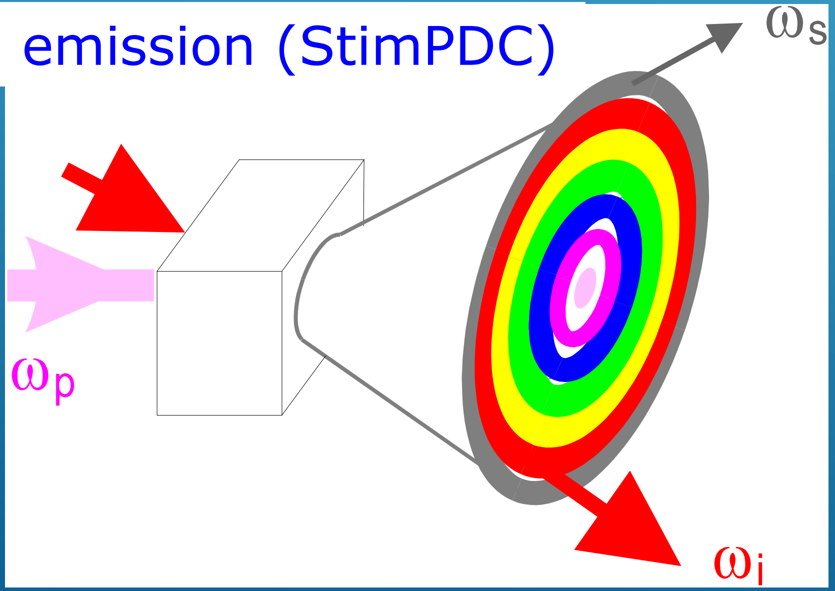

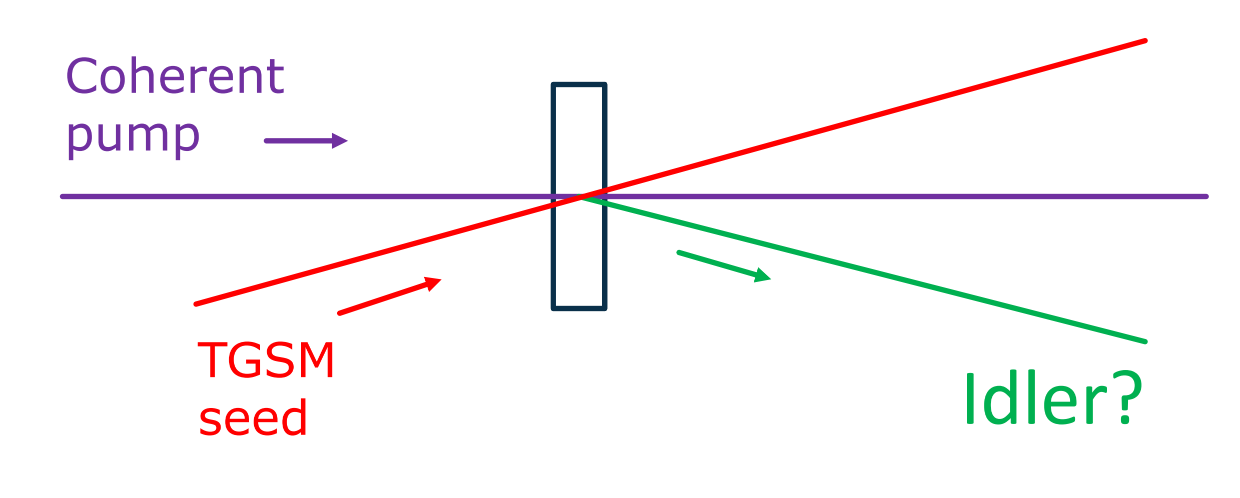

Partially coherent StimPDC

$$W_i(\mathbf{r},\mathbf{r}') = W_p(\mathbf{r},\mathbf{r}')W_s^*(\mathbf{r},\mathbf{r}').$$

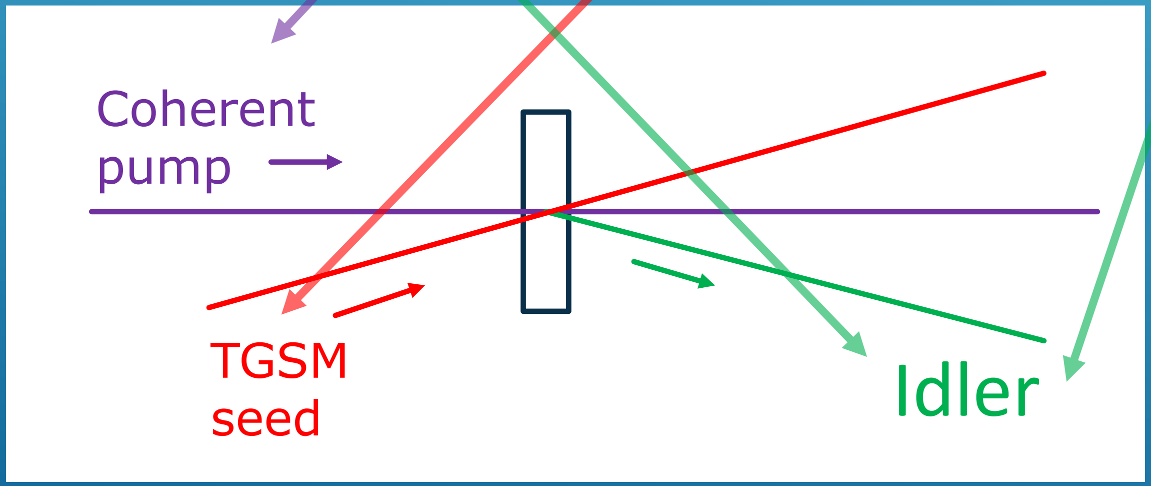

StimPDC with twisted Schell-model beams

$$W_i(\mathbf{r},\mathbf{r}') = A e^{-\frac{r^2+r'^2}{4w_i^2}} e^{-\frac{(\mathbf{r}-\mathbf{r}')^2}{2\delta_i^2}} e^{-ik_i\frac{(\mathbf{r}-\mathbf{r}')^2}{2R_i}} e^{-ik_i\mu_i(xy'-yx')},$$

$$w_i^2 = \frac{w_s^2 w_p^2}{w_s^2 + w_p^2},$$

$$\delta_i^2 = \frac{\delta_s^2 \delta_p^2}{\delta_s^2 + \delta_p^2},$$

$$\frac{k_i}{R_i} = \frac{k_p}{R_p} - \frac{k_s}{R_s},$$

$$k_i\mu_i = k_p\mu_p - k_s\mu_s,$$

Experiment

Pump @ 405 nm
Seed @ 780 nm
Idler @ 840 nm

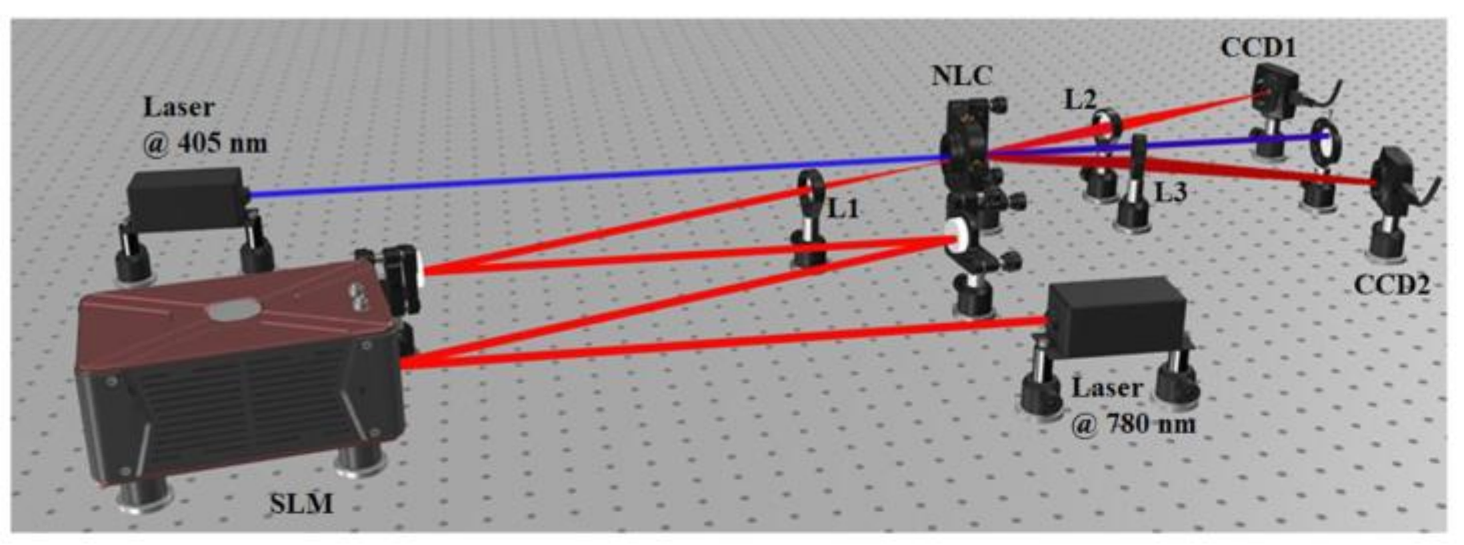

Results

Far field variance

$$\sigma_{\text{ff}}^2 = \left(\frac{1}{4w^2} + \frac{k^2 w^2}{R^2}\right) + \frac{1}{\delta^2} + \frac{\tau^2 w^2}{\delta^4},$$

Far field variance x degree of coherence

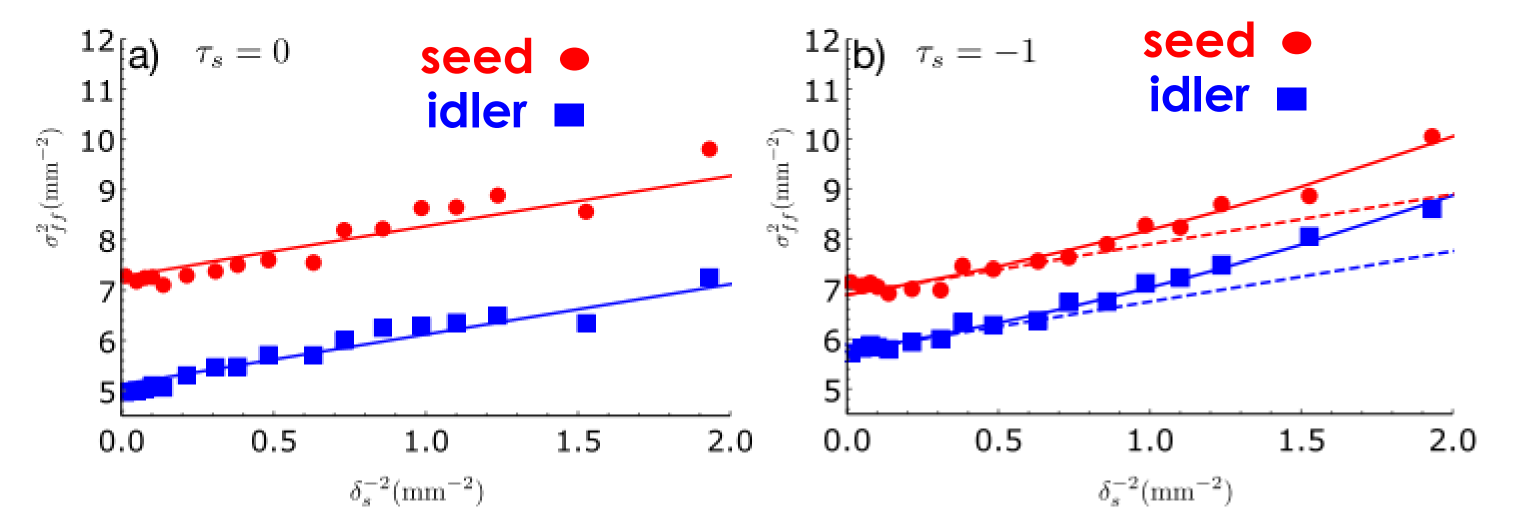

Visibility in a double-slit interference

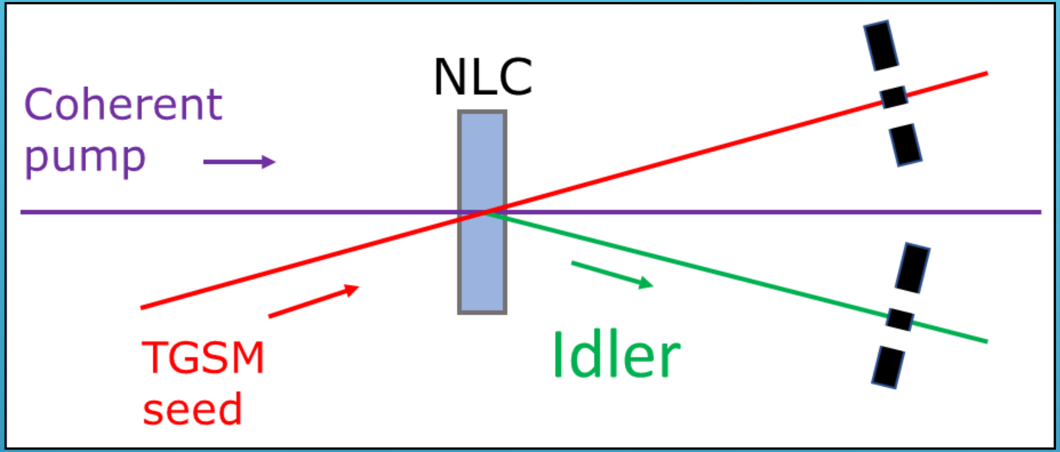

Visibility x degree of coherence

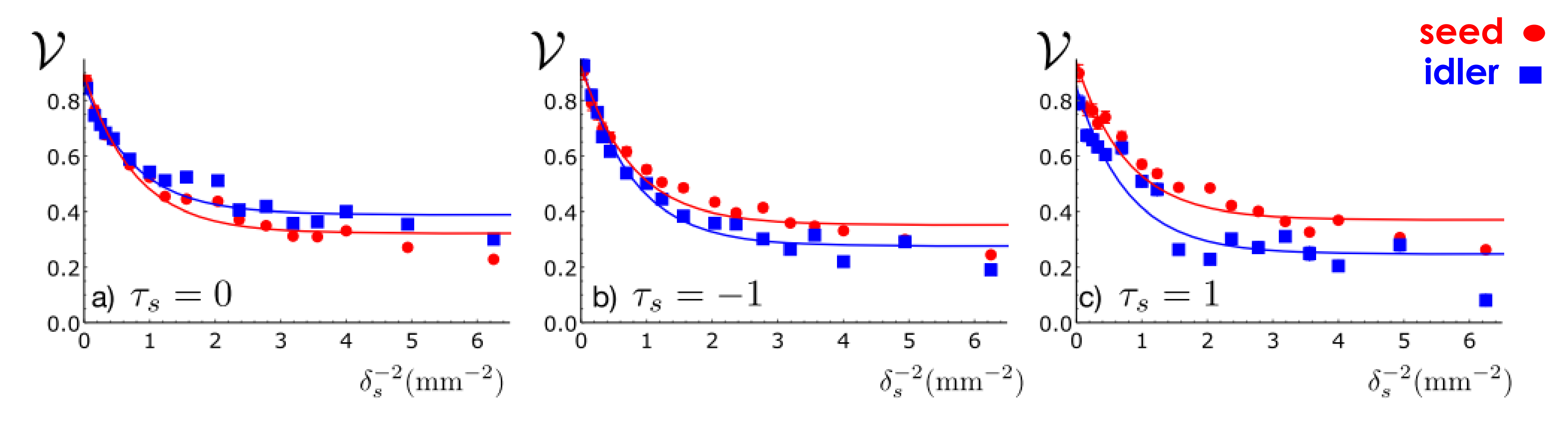

Transfer and conjugation of twist phase

$$I(\mathbf{r}) \approx \left[1 + e^{-\frac{2d^2}{\delta^2}} \cos\left\{2dk\left(\frac{y}{f} - \mu x\right)\right\}\right]$$

Twist in the fringe pattern

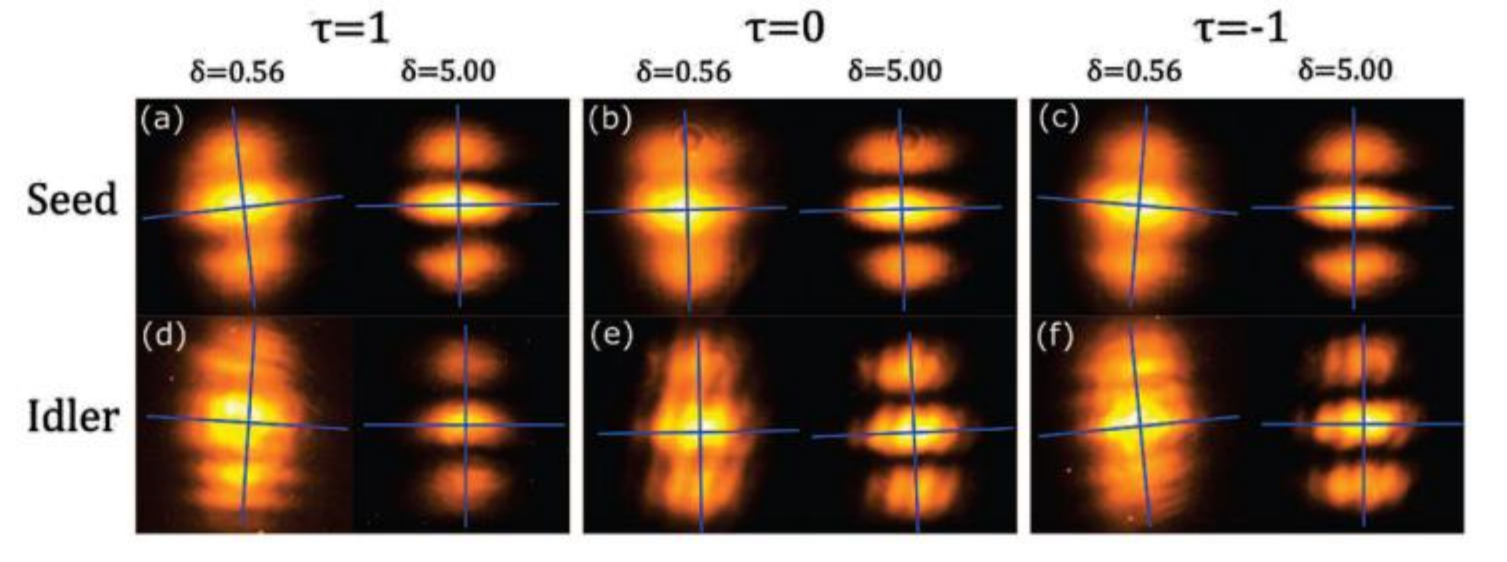

IOP Publishing Journal of Optics
J. Opt. 24 (2022) 094004 (8pp) https://doi.org/10.1088/2040-8986/ac8562

Evaluation of twisted Gaussian Schell model beams produced with phase randomized coherent fields

G Cañas[1,2], E S Gómez[2,3], G H dos Santos[4], A G de Oliveira[4], N Rubiano da Silva[4], Stuti Joshi[5], Yaseera Ismail[6], P H S Ribeiro[4,*] and S P Walborn[2,3,*]

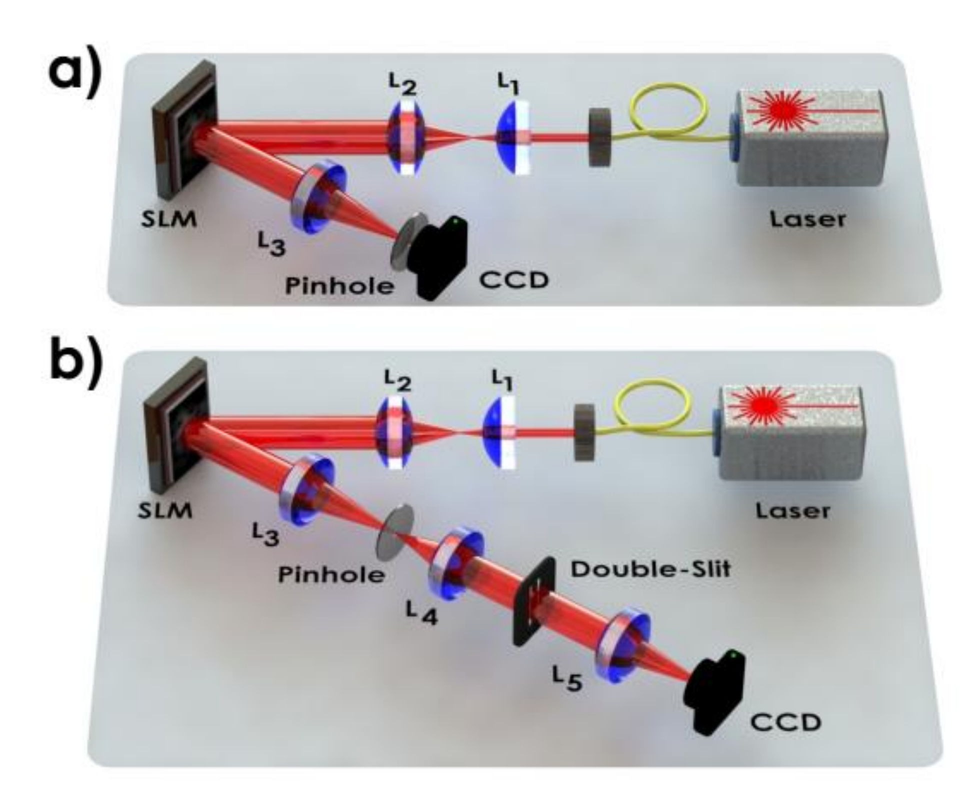

Far field mean variance versus coherence length

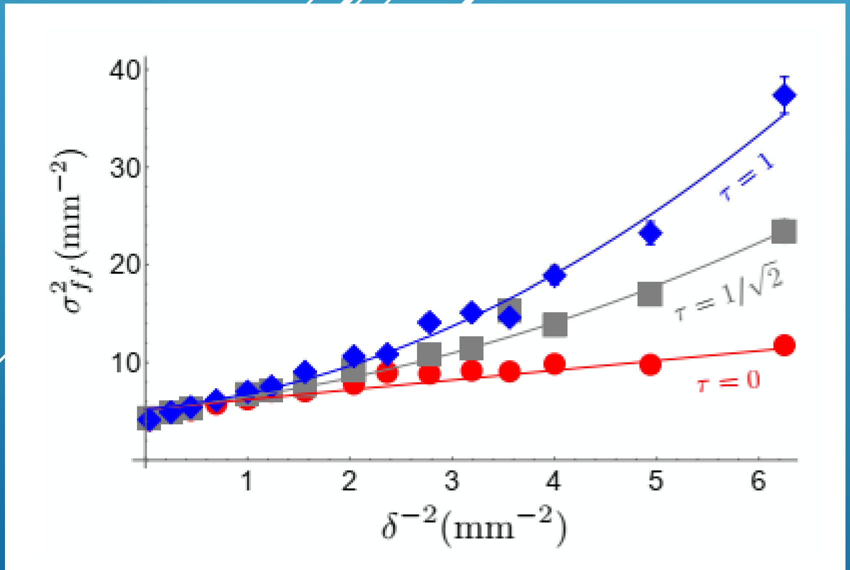

IOP Publishing Journal of Optics
J. Opt. 24 (2022) 094004 (8pp) https://doi.org/10.1088/2040-8986/ac8562

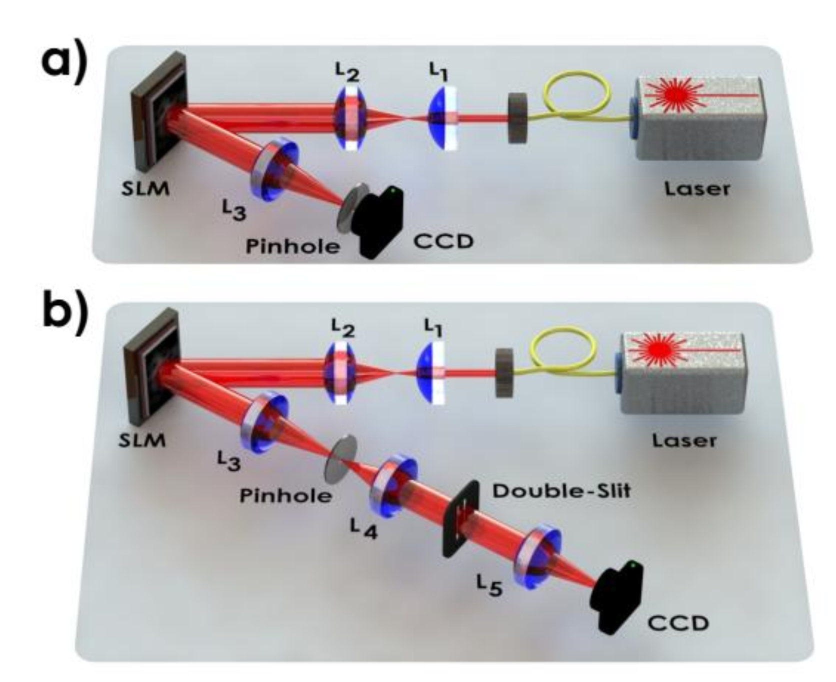

Residual coherence in SLM movie methods

τ = 0

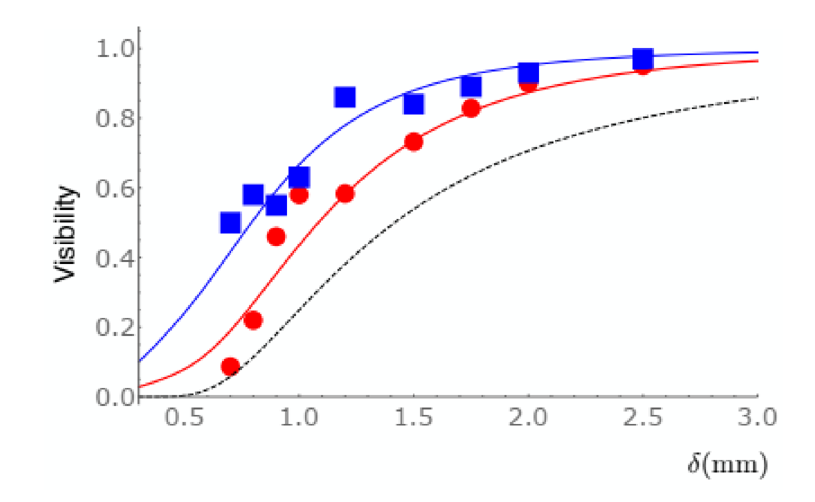

τ = 1

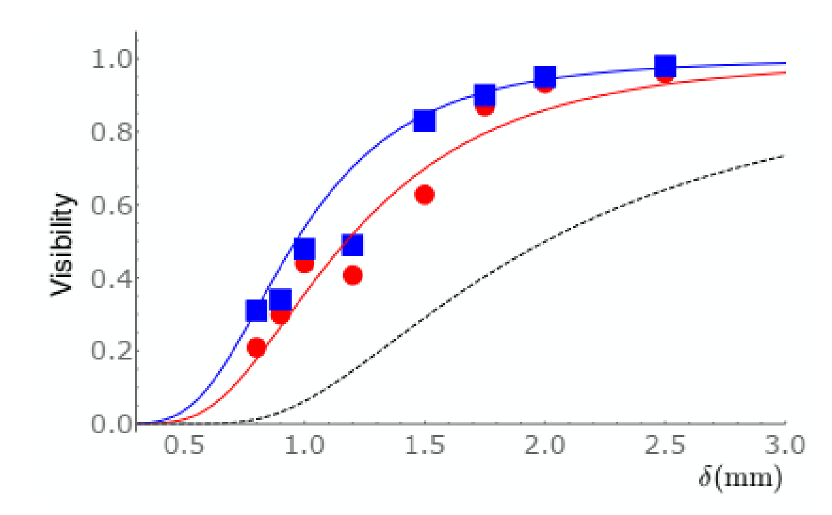

PHYSICAL REVIEW APPLIED **20**, 024007 (2023)

Partial Coherence and Coherence Length in Stimulated Parametric Down-Conversion

G.H. dos Santos,[1,*] R.C. Souza Pimenta,[1] R.M. Gomes,[2] S.P. Walborn,[3,4,†] and P.H. Souto Ribeiro[1,‡]

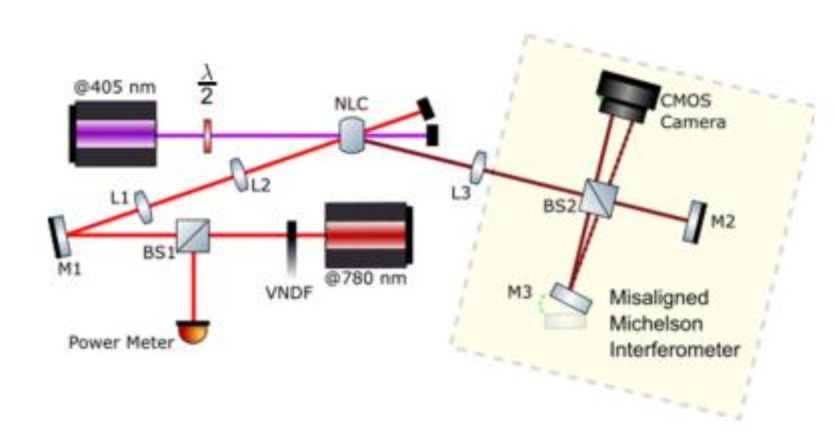

TABLE I. Normalized intensity of the stimulated component and ϵ-coherence lengths obtained for different seed beam intensities.

I_{seed} (μW)	β (%)	$\epsilon = 1/e$ (μm)	$\epsilon = 1/2$ (μm)	$\epsilon = 7/8$ (μm)
0	0	29.30	24.40	10.71
90	4.9 ± 3.5	30.64	25.32	11.00
270	13.9 ± 2.7	33.74	27.32	11.61
540	20.5 ± 2.5	36.88	29.17	12.12
3000	44.9 ± 1.8	∞	45.30	14.87
10 700	76.0 ± 1.7	∞	∞	25.12

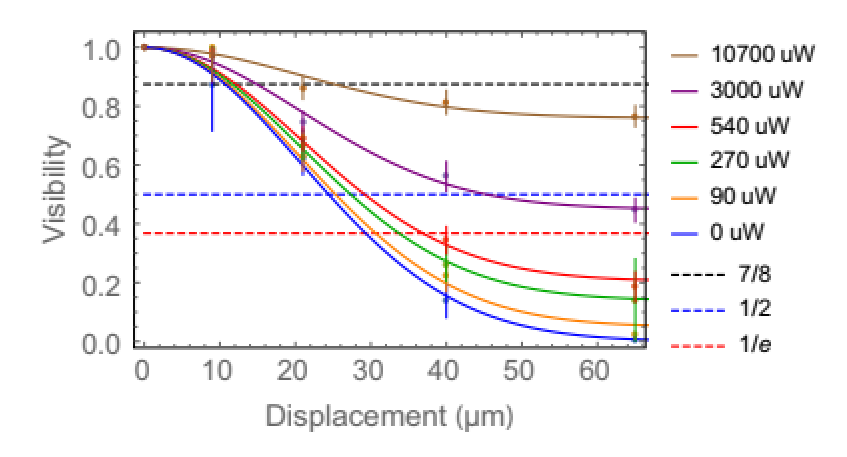

Contents lists available at ScienceDirect

Optics and Laser Technology

journal homepage: www.elsevier.com/locate/optlastec

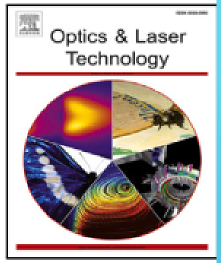

Full length article

Anomalous second harmonic generation of twisted Gaussian Schell model beams

M. Gil de Oliveira [a,*], A.L.S. Santos Junior [a], A.C. Barbosa [a], B. Pinheiro da Silva [a], G.H. dos Santos [b], G. Cañas [c,d], P.H. Souto Ribeiro [b], S.P. Walborn [c,e], A.Z. Khoury [a]

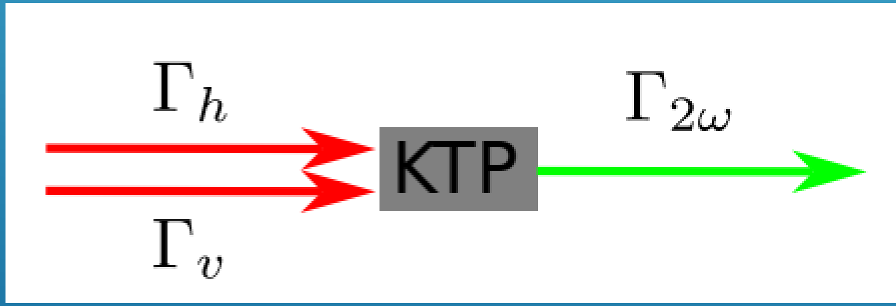

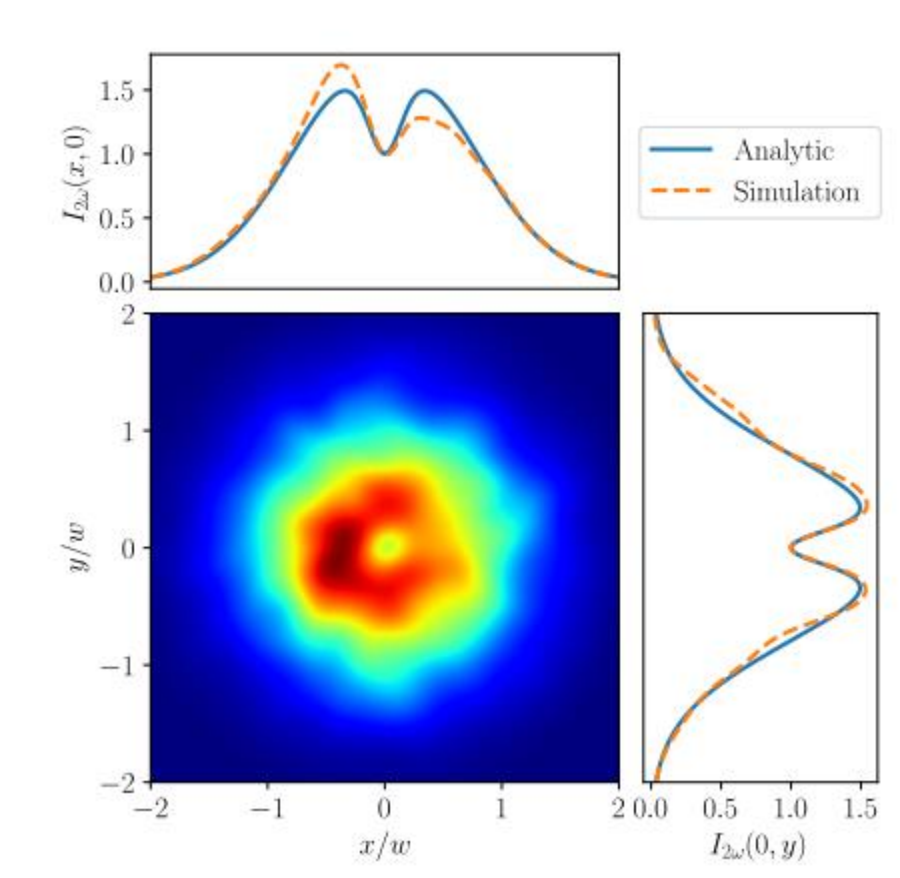

Contents lists available at ScienceDirect

Optics and Laser Technology

journal homepage: www.elsevier.com/locate/optlastec

Optics & Laser Technology

ELSEVIER

Full length article

Anomalous second harmonic generation of twisted Gaussian Schell model beams

M. Gil de Oliveira [a,*], A.L.S. Santos Junior [a], A.C. Barbosa [a], B. Pinheiro da Silva [a], G.H. dos Santos [b], G. Cañas [c,d], P.H. Souto Ribeiro [b], S.P. Walborn [c,e], A.Z. Khoury [a]

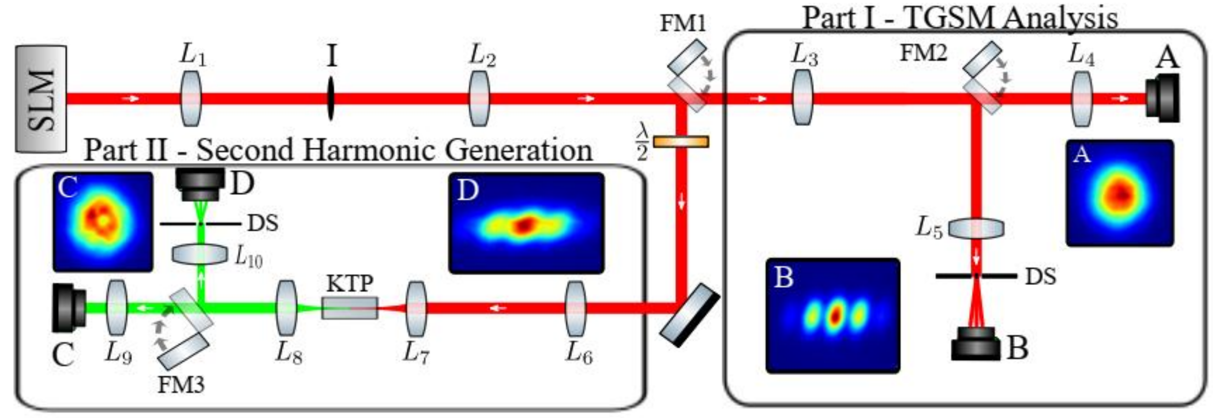

Figure 4: Experimental setup.

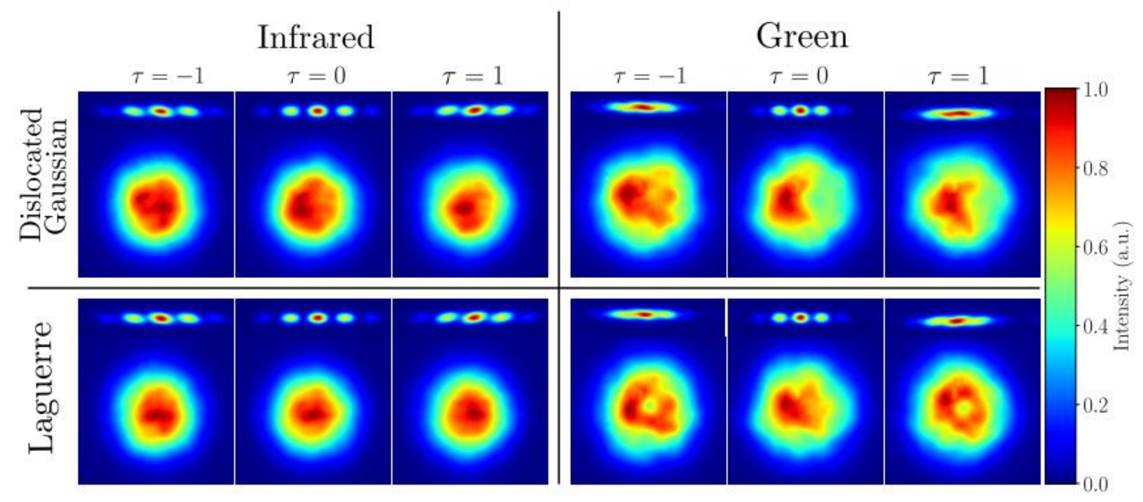

Conclusions

Partial coherence GSM and TGSM beams

TGSM beams: applications to communication through turbulent medium

TGSM and SPDC applications to quantum systems

TGSM and wavelength conversion in StimPDC

StimPDC as a design for SPDC experiments in quantum regime

Perspectives

Testing twist conservation in nonlinear parametric interactions

Testing experimentally the use of TGSM to boost the entanglement

Using TGSM beams in optical communication
REDE RIO QUÂNTICA (A. Z. Khoury)

Floripa

Thank you!